

AD-A082 984

NAVAL OCEAN RESEARCH AND DEVELOPMENT ACTIVITY NSTL S-ETC P/B 8/10  
SOUND SPEED AND OCEANIC FRONTRAL VARIABILITY IN THE WESTERN ALBO-ETC(U)  
SEP 79 D F PEDDER  
NORDA-TN-82

UNCLASSIFIED

RL

100-1  
AD-A082 984  
[Redacted]

END  
DATE FILMED  
5-80  
DTIC

LEVEL

12

NORDA TECHNICAL NOTE 52

9

SOUND SPEED AND OCEANIC FRONTAL VARIABILITY  
IN THE WESTERN ALBORAN SEA  
(JANUARY-MARCH 1979)

ADA 082984

10 DON F. FENNER

DTIC  
SELECTED  
APR 10 1980  
S C D

Ocean Acoustics Division  
OCEAN SCIENCE TECHNOLOGY LABORATORY



11 September 1979

12 42

14 NORDA-TN-52

This document has been approved  
for public release and sale; its  
distribution is unlimited.

Distribution Unlimited

NAVAL OCEAN SCIENCES AND UNDERWATER ACOUSTICS

NAVAL OCEAN SCIENCES AND UNDERWATER ACOUSTICS

392793

4 9 078

DC FILE COPY

## EXECUTIVE SUMMARY

This report contains an interpretation of temperature and sound speed data collected between 26 January and 19 March 1979 in the western Alboran Sea as part of a Fleet exercise. Analysis of these data during four separate periods (1-4, 10, and 19 February and 2-3 March) indicates:

- o The Alboran Front (centered about the 15°C isotherm at a depth of 100 m) was the major oceanographic feature affecting sound speed variability.
- o A warm, anticyclonic eddy of Atlantic Water (bounded on the north by the Alboran Front) occupied most of the western Alboran Sea between 26 January and 2-3 March, but was absent west of 40°30'W on 10-11 March.
- o The Alboran Frontal Zone (defined as the region between the 14° and 16°C isotherms at 100 m) varied in width between 3 nm (6 km) and about 20 nm (37 km) during the exercise.
- o Sonic layer depth was typically 120-180 m within the anticyclonic gyre and less than 40-60 m north of the Alboran Frontal Zone. Sonic layer depth gradients across the frontal zone were as great as 16.7 m/nm (9.1 m/km).
- o Anomalously shallow sonic layer depths (40-80 m) frequently occurred south of the Alboran Frontal Zone, and were probably caused by an injection of colder, upwelled water from north of the front into the surface mixed layer.
- o The depth of the deep sound channel axis was typically 200-250 m within the anticyclonic eddy and 100-150 m north of the Alboran Frontal Zone. Deep axial depth gradients across the frontal zone were as great as 15.0 m/nm (8.3 m/km).
- o Depth excess throughout the exercise area was more than adequate for convergence zone propagation from either a near-surface or a 100 m source.
- o Maximum spatial variability in sound speed along 40°30'W (meridional section) on four separate days and maximum temporal variability in sound speed near the center of the section (at 36°N) between 26 January and 19 March were of the same magnitude (about 11 m/sec) and occurred at approximately the same depth (about 125 m). Suspected causative phenomena include air-sea interaction, frontal meandering, and upwelling along the northern edge of the anticyclonic gyre.
- o Atmospheric forcing was observed to affect both the size and location of the anticyclonic eddy. Lower atmospheric pressures caused a larger eddy located in a more easterly position, while higher pressures caused a smaller eddy located closer to the Strait of Gibraltar.

## CONTENTS

	PAGE
LIST OF ILLUSTRATIONS	iv
LIST OF TABLES	v
I. INTRODUCTION	1
II. OCEANOGRAPHIC DATA	1
III. GENERAL OCEANOGRAPHIC SETTING	4
IV. OCEANOGRAPHIC CONDITIONS ON 1-4 FEBRUARY	4
V. OCEANOGRAPHIC CONDITIONS ON 10 FEBRUARY	8
VI. OCEANOGRAPHIC CONDITIONS ON 19 FEBRUARY	16
VII. OCEANOGRAPHIC CONDITIONS ON 2-3 MARCH	16
VIII. SUMMARY OF TEMPORAL AND SPATIAL VARIABILITY ALONG NORTH-SOUTH TRACK	23
IX. TEMPORAL VARIABILITY IN SOUND SPEED AT 36°00'N, 40°28'W	23
X. TEMPORAL VARIABILITY OF ALBORAN FRONT AND ANTICYCLONIC EDDY	27
XI. SUMMARY	30
XII. REFERENCES	32

Accession For	
NTIS GRAIL	
DDC TAB	
Unannounced	
Justification	
By	
Distribution/	
Availability Codes	
Dist	Available and/or special
A	

## ILLUSTRATIONS

	Page
Figure 1. Location of Oceanographic Data (26 January-19 March 1979)	3
Figure 2. Temperature-Salinity-Sound Speed Comparison for RESEARCHER STD 4 (3 March 1979)	5
Figure 3. Location of 1 and 4 February XBT/AXBT Data	6
Figure 4. Temperature and Sound Speed Parameters on 4 February	7
4a. Sea Surface Temperature	
4b. Sonic Layer Depth	
4c. Temperature at 100 m	
4d. Depth of Deep Sound Channel Axis	
Figure 5. Sound Speed Cross-Section Along 1 February North-South Track	9
Figure 6. Sound Speed Composite Along 1 February North-South Track	10
Figure 7. Location of 10 February AXBT Data	11
Figure 8. Temperature and Sound Speed Parameters on 10 February	13
8a. Sea Surface Temperature	
8b. Sonic Layer Depth	
8c. Temperature at 100 m	
8d. Depth of Deep Sound Channel Axis	
Figure 9. Sound Speed Cross-Section Along 10 February North-South Track	14
Figure 10. Sound Speed Composite Along 10 February North-South Track	15
Figure 11. Location of 19 February AXBT Data	17
Figure 12. Temperature and Sound Speed Parameters on 19 February	18
12a. Sea Surface Temperature	
12b. Sonic Layer Depth	
12c. Temperature at 100 m	
12d. Depth of Deep Sound Channel Axis	
Figure 13. Sound Speed Cross-Section Along 19 February North-South Track	19
Figure 14. Sound Speed Composite Along 19 February North-South Track	20
Figure 15. Location of 2-3 March STD/XBT Data	21
Figure 16. Sound Speed Cross-Section Along 2-3 March North-South Track	22
Figure 17. Sound Speed Composite Along 2-3 March North-South Track	24
Figure 18. Comparison of Sound Speed Parameters Along North-South Track	25

	Page
Figure 19. Temporal Variability in Sound Speed Near Center of North-South Track	26
Figure 20. Mean Position of Alboran Front at 100 m (24 January - 11 March 1979)	28

#### TABLES

Table 1. Summary of Oceanographic Data	2
--	---

## I. INTRODUCTION

During January through March 1979, a Fleet-oriented exercise was conducted in the western Alboran Basin of the Mediterranean Sea (west of about  $30^{\circ}30'W$ ). The research and development support for this exercise was provided by the Naval Ocean Research and Development Activity (NORDA) and the Naval Underwater Systems Center, New London Laboratory (NUSC/NL). NORDA coordinated the oceanographic data collection portion of the exercise, which included support from the Naval Oceanographic Office (NAVOCEANO), the National Oceanic and Atmospheric Administration (NOAA), and Maritime Patrol Squadrons VP-11 and VP-16. The Environmental Effects Branch, Ocean Acoustics Division of NORDA, had primary responsibility for analyzing oceanographic data to support acoustic analysis. This report documents the oceanographic conditions that occurred during the exercise in terms of sound speed variability (both temporal and spatial) and the position of the Alboran Front, the major oceanographic feature of the western Alboran Sea.

## II. OCEANOGRAPHIC DATA

Table 1 summarizes the oceanographic data collected during the exercise in terms of date, collecting platform, and data type. Most of the exercise data base consisted of AN/SSQ-36 airborne expendable bathythermographs (AXBTs) that sample to a maximum depth of 330 m. These data were collected by the NAVOCEANO Aircraft Squadron (VXN-8) and Squadrons VP-11 and VP-16. Expendable bathythermograph (XBT) data were collected by the USNS HARKNESS toward the beginning of the exercise (1 February) and by the NOAA Ship (NS) RESEARCHER toward the end of the exercise (2-3 March). Both ships used Sippican Model T-4 XBT probes (maximum rated depth of 450 m). RESEARCHER also collected oceanographic data using a Plessy Model 9040 STD (salinity-temperature-depth) system and bathymetric data using a narrow-beam echo-sounder.

All oceanographic data collected during the exercise were converted to sound speed using the equation of Mackenzie (1976 and 1977). Salinities necessary for sound speed calculation were individually assigned to each AXBT or XBT profile, and were based on the salinity field derived from historical data collected by R/V CHAIN in February 1975 (Bryden et al., 1978) and USNS KANE in January 1977 (unpublished NAVOCEANO data from KANE Cruise No. 343714). RESEARCHER STD data were converted to sound speed using in situ salinities. The AN/SSQ-36 AXBT, with a temperature accuracy of  $\pm 0.3^{\circ}\text{C}$ , yields calculated sound speeds accurate to about  $\pm 1.2 \text{ m/sec}$ , providing that proper salinities are assigned to each AXBT profile. The Sippican Model T-4 XBT measures temperature to  $\pm 0.2^{\circ}\text{C}$ , which results in a calculated sound speed accuracy of about  $\pm 0.8 \text{ m/sec}$ , providing salinities are correctly assigned. The Plessy Model 9040 STD used during the exercise measures temperatures accurate to  $\pm 0.02^{\circ}\text{C}$  and salinities accurate to  $\pm 0.02^{\circ}/\text{oo}$ , resulting in calculated sound speeds accurate to about  $\pm 0.1 \text{ m/sec}$ .

Figure 1 shows the location of all useful oceanographic data collected during the exercise. By design, oceanographic data were collected along about  $40^{\circ}30'W$  (meridional section) on 1, 4, 10, and 19 February and on 2-3 March. By chance, some AXBT, XBT, and STD data clustered within about 6 nm (11 km) of  $36^{\circ}00'N$ ,  $40^{\circ}28'W$  over the course of the exercise. The circle near the center of Figure 1 denotes the location of these data, which are presented as a sound speed composite later in this report (Fig. 19). The overall distribution of oceanographic data was more than adequate to define environmental effects on acoustic propagation, and lends itself readily to both areal and vertical contouring.

TABLE 1  
SUMMARY OF OCEANOGRAPHIC DATA

DATE (1979)	PLATFORM	AXBTs	XBTs	STDs
24 JAN	VXN-8	24	--	--
26 JAN	VXN-8	23	--	--
01 FEB	USNS HARKNESS	--	24	--
04 FEB	VP-11	31	--	--
09 FEB	VP-16	10	--	--
10 FEB	VP-11	32	--	--
19 FEB	VP-11	36	--	--
2-3 MAR	NS RESEARCHER	--	24	6
10 MAR	VP-11	12	--	--
11 MAR	VXN-8	10	--	--
19 MAR	VXN-8	5	--	--
TOTALS		183	48	6

NOTE: Statistics reflect those observations adjudicated useful, not total observations taken by a given platform.

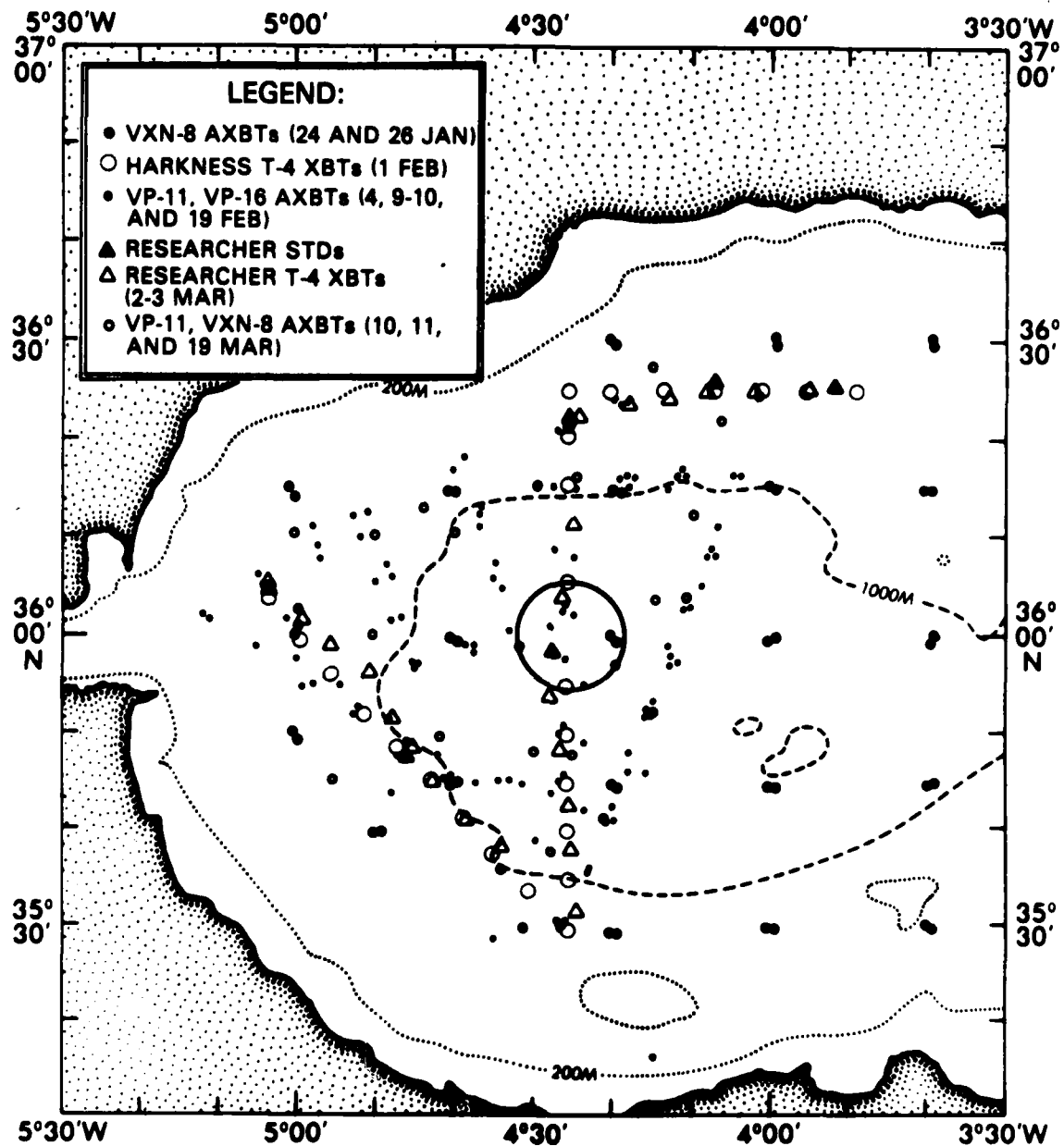


Figure 1. Location of oceanographic data (26 January-19 March 1979)

### III. OCEANOGRAPHIC SETTING

One of the most pronounced fronts in the Mediterranean occurs in the western Alboran Sea, just inside the Strait of Gibraltar. Referred to as the Alboran Front, this oceanic frontal zone separates an anticyclonic (clockwise) gyre of warm, lower salinity Atlantic Water emanating through the Strait of Gibraltar from cooler, higher salinity Mediterranean Water resident in the Alboran Sea. The anticyclonic gyre and the associated Alboran Front have been documented during summer (July-September) by Lanoix (1974) and Ovchinnikov et al. (1976), during autumn (October) by Cheney and Doblar (1979), and during winter (January-March) by Cheney (1977, 1978). The frontal zone is confined to the upper 200-250 m of the water column, has horizontal temperature difference of 2-4°C at 100 m, and has a typical width of 20 nm (37 km). During winter, the axis (or mean position) of the front corresponds to the 17°C isotherm at the surface and the 15°C isotherm at a depth of 100 m. The anticyclonic gyre apparently is a persistent feature in the western Alboran Sea throughout the year, and the Alboran Front appears to be coherent from Gibraltar west to about 10°W (Cheney, 1978). Under proper weather conditions, the surface expression of the front can be seen clearly in satellite infrared imagery.

Below a depth of 200-250 m, the circulation of the western Alboran Sea is basically cyclonic (counterclockwise) and is dominated by the flow of Levantine Intermediate Water with a high salinity core at 400-500 m. Wust (1961) shows an east-west flow of Levantine Intermediate Water along about 35°30'W. However, more recent work of Ovchinnikov et al. (1976) indicates that the high salinity flow enters the Alboran Sea along the Iberian Coast and is caught up in a generally cyclonic transport that extends to depths greater than 1000 m. Below a depth of about 600 m, both temperature and salinity are extremely stable throughout the western Alboran Sea (12.9-13.0°C and 38.42-38.45‰, respectively).

Figure 2 presents profiles of temperature, salinity, and sound speed, plus a T-S diagram for an STD station taken by RESEARCHER on 3 March at about 36°00'N, 4°29'W. Sonic layer depth (the depth of the near-surface sound speed maximum) corresponds to the maximum depth of winter cooling. The depth of the deep sound channel axis (i.e., the depth of the absolute sound speed minimum) coincides with the bottom of the permanent thermocline and generally defines the lower boundary of the anticyclonic eddy. The depth of the high salinity Levantine Intermediate Water core is marked by a slight temperature and salinity maximum. The profiles presented in Figure 2 are representative of winter oceanographic conditions near the center of the western Alboran Sea anticyclonic eddy.

### IV. OCEANOGRAPHIC CONDITIONS ON 1-4 FEBRUARY

Figure 3 shows the location of HARKNESS T-4 XBT data collected on 1 February plus AXBT data collected on 4 February as part of a VP-11 flight. Oceanographic conditions during the first four days of February were generally similar throughout most of the exercise area. HARKNESS XBT data used in the meridional sound speed cross-section (north-south track) also are identified in Figure 3.

Figure 4 shows contoured presentations of sea surface temperature, sonic layer depth, temperature at 100 m, and the depth of the deep sound channel axis based on all data collected by VP-11 on 4 February. At the surface (Fig. 4a), the total temperature contrast was less than 1.5°C, and the Alboran Front was not discernable. At a depth of 100 m (Fig. 4c), the axis of the Alboran Front corresponded to the 15°C isotherm (by definition), and generally followed the position of the 1000 m bathymetric contour in the region west of about 4°50'W. The width of the frontal zone (defined as the distance between the 14°C and 16°C

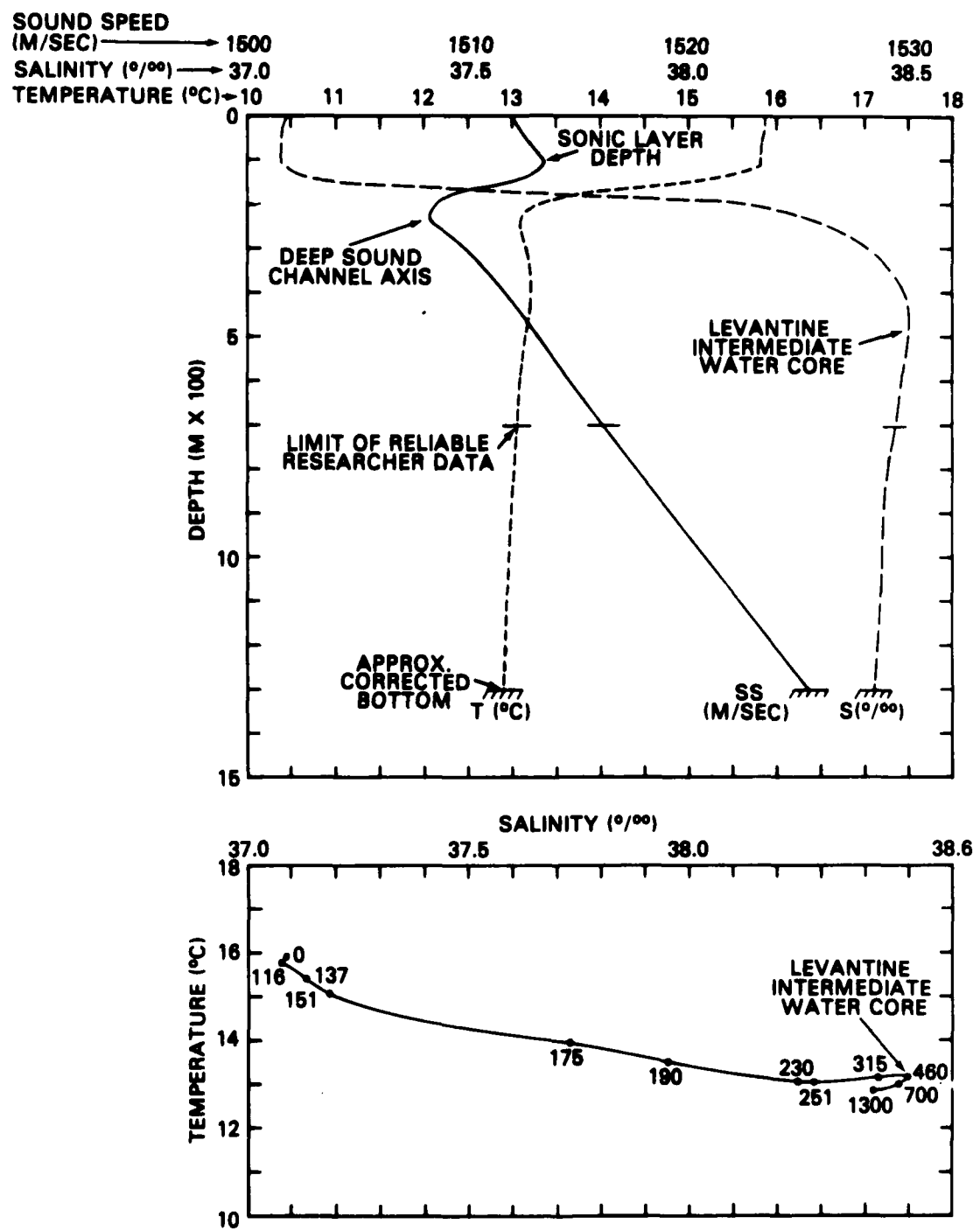


Figure 2. Temperature-salinity-sound speed comparison for RESEARCHER STD 4 (3 March 1979)

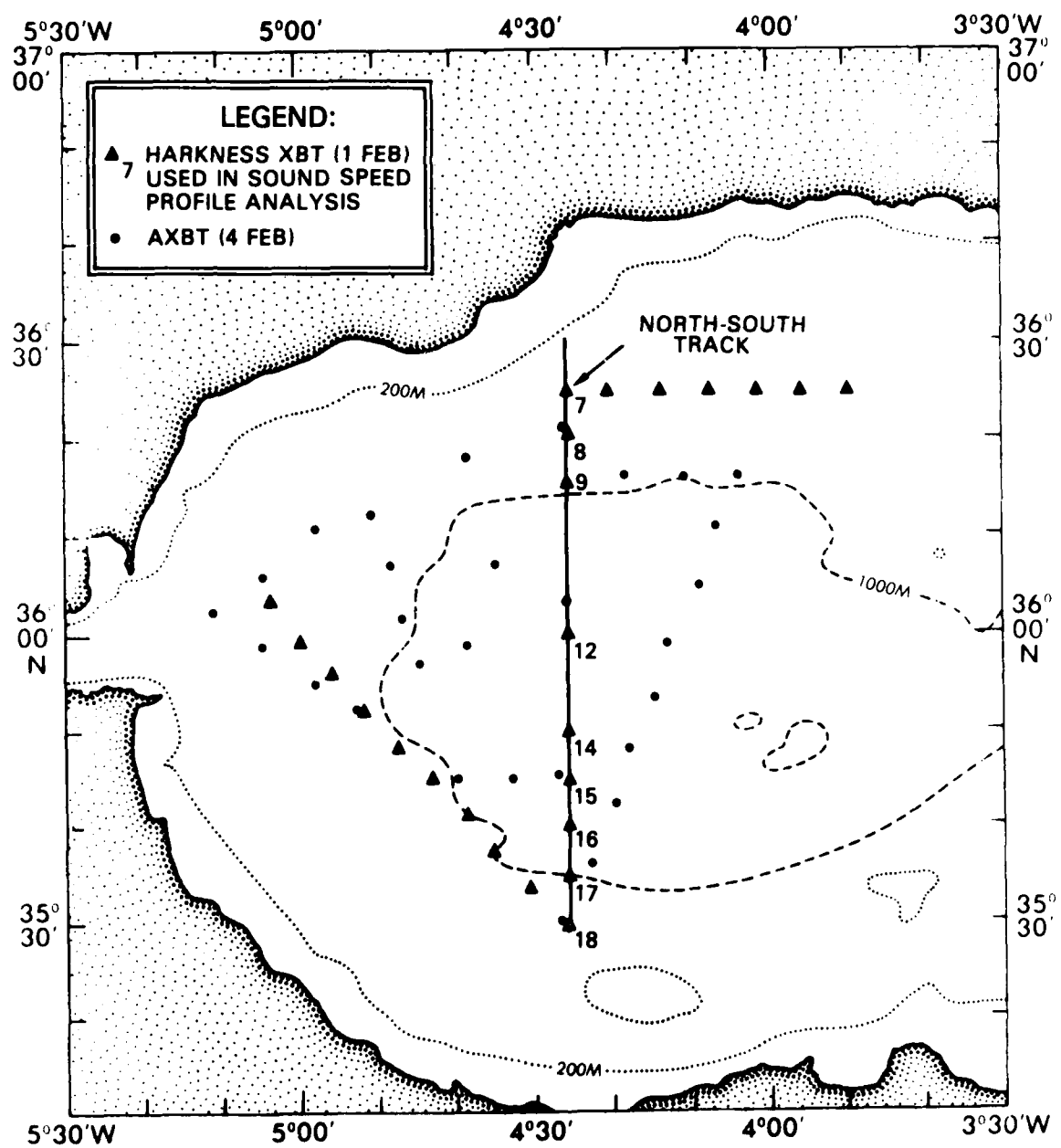


Figure 3. Location of 1 and 4 February XBT/AXBT data

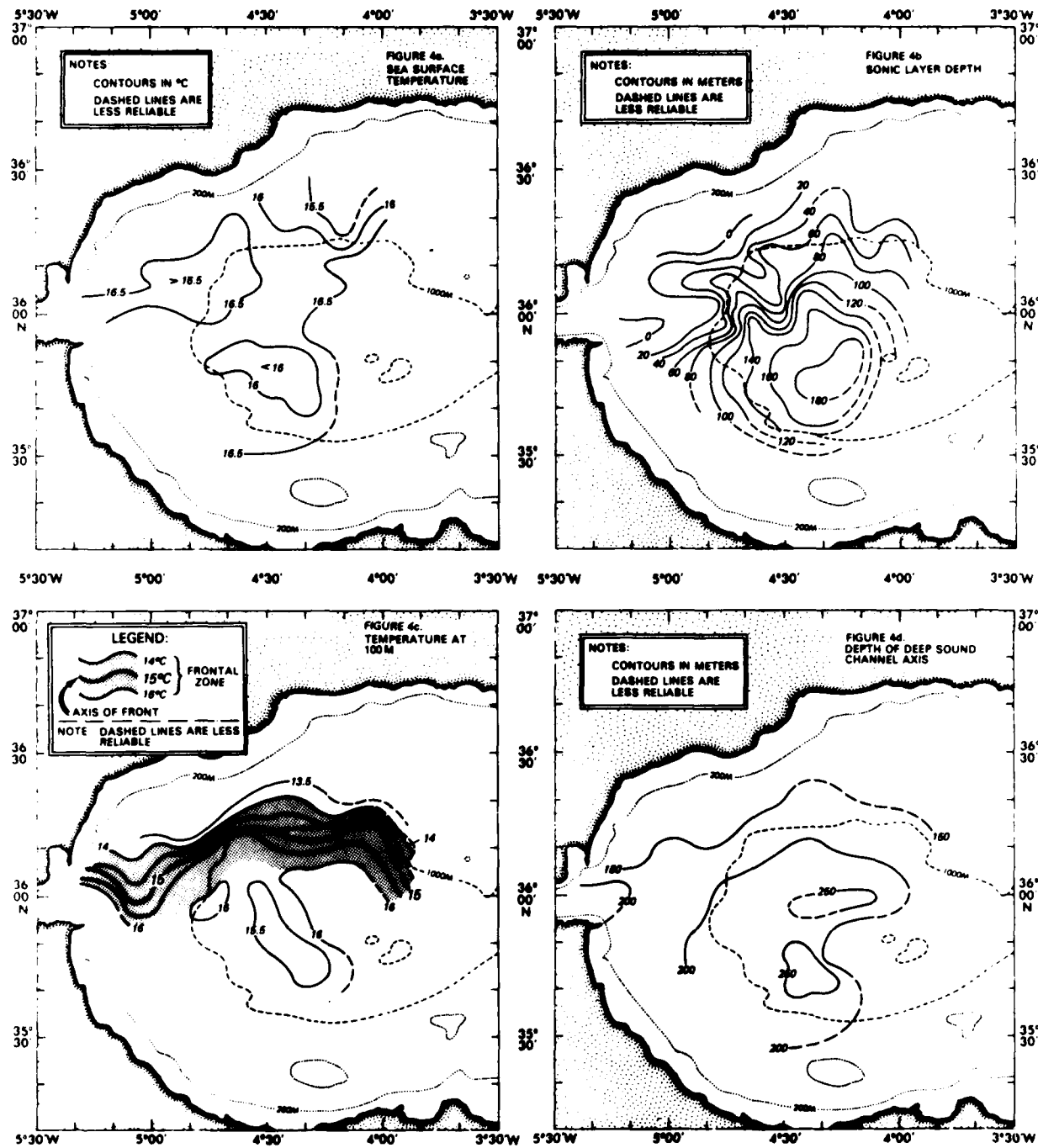


Figure 4. Temperature and sound speed parameters on 4 February

isotherms measured normal to the frontal axis) varied from about 18 nm (33 km) along  $5^{\circ}\text{W}$  to 10 nm (18 km) along  $40^{\circ}40'\text{W}$  and  $40^{\circ}10'\text{W}$ .

Sonic layer depth on 4 February (Fig. 4b) varied from greater than 180 m near the center of the anticyclonic gyre to 0 m (surface) in the region north of the Alboran Front. The maximum horizontal gradient in sonic layer depth occurred along about  $36^{\circ}\text{N}$  between about  $40^{\circ}40'\text{W}$  and  $40^{\circ}50'\text{W}$ . Here, the sonic layer changed by 120 m over a distance of about 6 nm (11 km). This region of rapid change occurred south of the southern edge of the Alboran Frontal Zone and did not correspond well with the mean position of the Alboran Front at 100 m. This situation is anomalous compared to that found during January and March 1977, when the maximum horizontal gradient in sonic layer depth corresponded well with the axis of the Alboran Front (Cheney, 1977). In the case of the 4 February data, the axis of the front generally corresponded to sonic layer depths of less than 80 m. Shallower sonic layer depths south of the Alboran Front axis on 4 February may have been caused by injection of colder water from north of the front into the surface mixed layer, probably as a result of upwelling along the northern edge of the anticyclonic gyre. Such an injection is indicated by the convoluted form of the sonic layer depth isopleths along the northern edge of the gyre.

The depth of the deep sound channel axis on 4 February (Fig. 4d) varied from greater than 250 m in the center of the gyre to less than 150 m north of the Alboran Front. The 150 and 200 m axial depth contours corresponded to the position of the frontal zone, a situation analogous to that reported by Cheney (1977).

Figure 5 shows a contoured sound speed cross-section along the 1 February north-south track. Data spacing along the 1 February track was wider than desired, but was considerably better than that during the 4 February VP-11 overflight (Fig. 3). An overplot of selected sound speed profiles along the 1 February meridional cross-section is presented in Figure 6. The track intersected the Alboran Frontal Zone between  $36^{\circ}$  and  $36^{\circ}15'\text{N}$  (i.e., between ranges of 30-45 nm or 56-83 km). Exact details of sound speed variability across the Alboran Front are obscured by lack of samples within the frontal zone. The axis of the deep sound channel shoaled to the north across the frontal zone, as did sonic layer depth. However, the most rapid change in sonic layer depth occurred just south of the frontal zone between ranges of 20 and 30 nm (37 and 56 km). Here, the sonic layer shoaled from 145 to 75 m (gradient of 7.0 m/nm or 3.7 m/km). Along the section as a whole, the greatest lateral sound speed variability (nearly 10 m/sec) occurred at a depth of 160 m (Fig. 6).

The entire 1 February meridional section was deeper than either critical depth or 100 m conjugate depth. Critical depth, that depth where the maximum sound speed at the surface or in the surface mixed layer recurs, defines the bottom of the deep sound channel. The depth where sound speed at 100 m recurs is defined as 100 m conjugate depth, and delineates the minimum depth necessary for refraction of downward rays from a 100 m source. Neither critical nor 100 m conjugate depth shoaled markedly across the Alboran Frontal Zone. However, the 100 m conjugate depth shoaled rapidly in the region north of  $36^{\circ}15'\text{N}$ . On 1 February, depth excess (the difference between critical or 100 m conjugate depth and corrected bottom depth) was adequate along the entire track to support convergence zone propagation from sources at all depths above critical depth.

#### V. OCEANOGRAPHIC CONDITIONS ON 10 FEBRUARY

Figure 7 shows the location of AXBT data collected on 10 February as a part of VP-11 flight. This figure also identifies AXBT data used in the 10 February

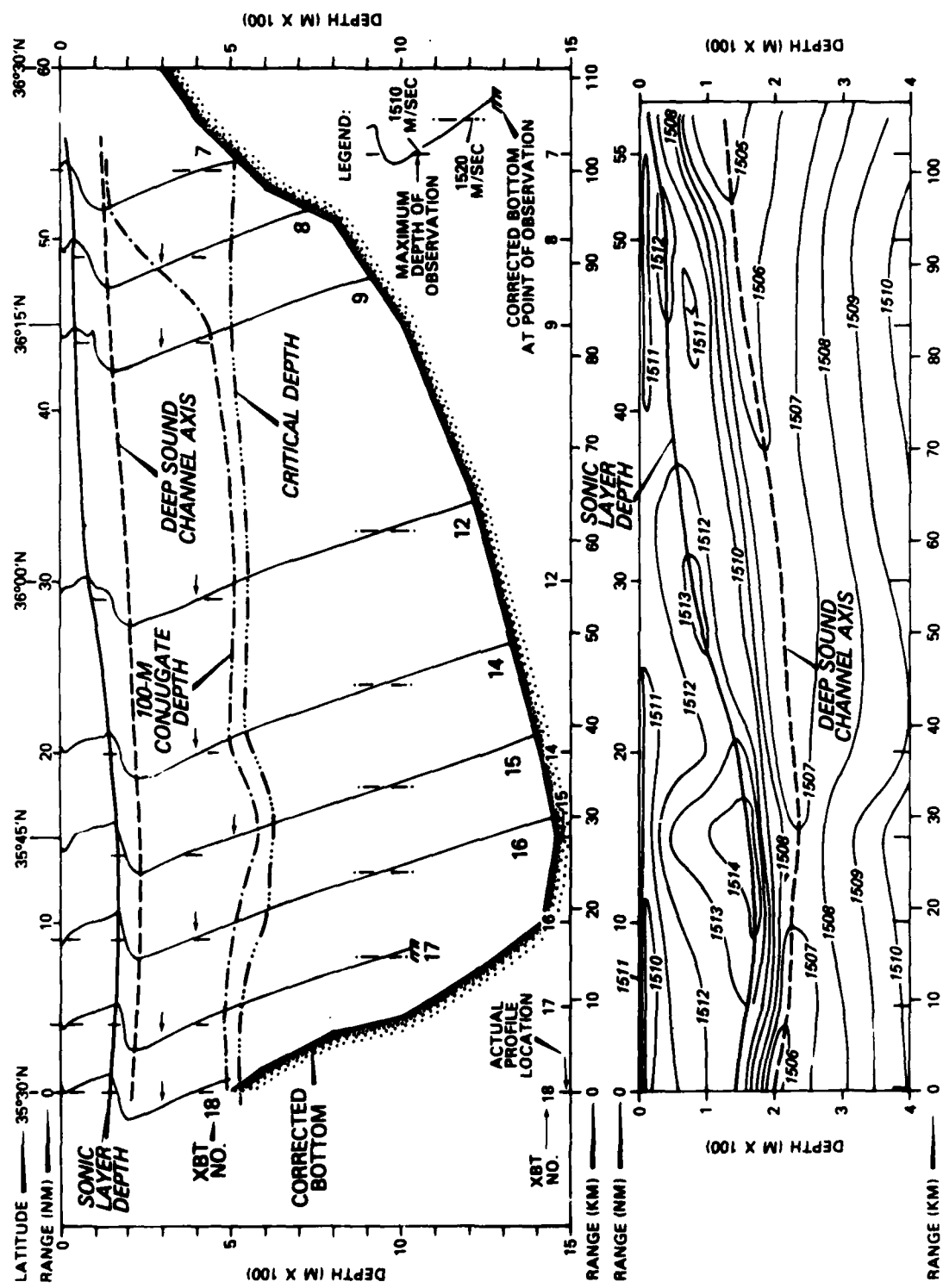


Figure 5. Sound speed cross section along 1 February north-south track

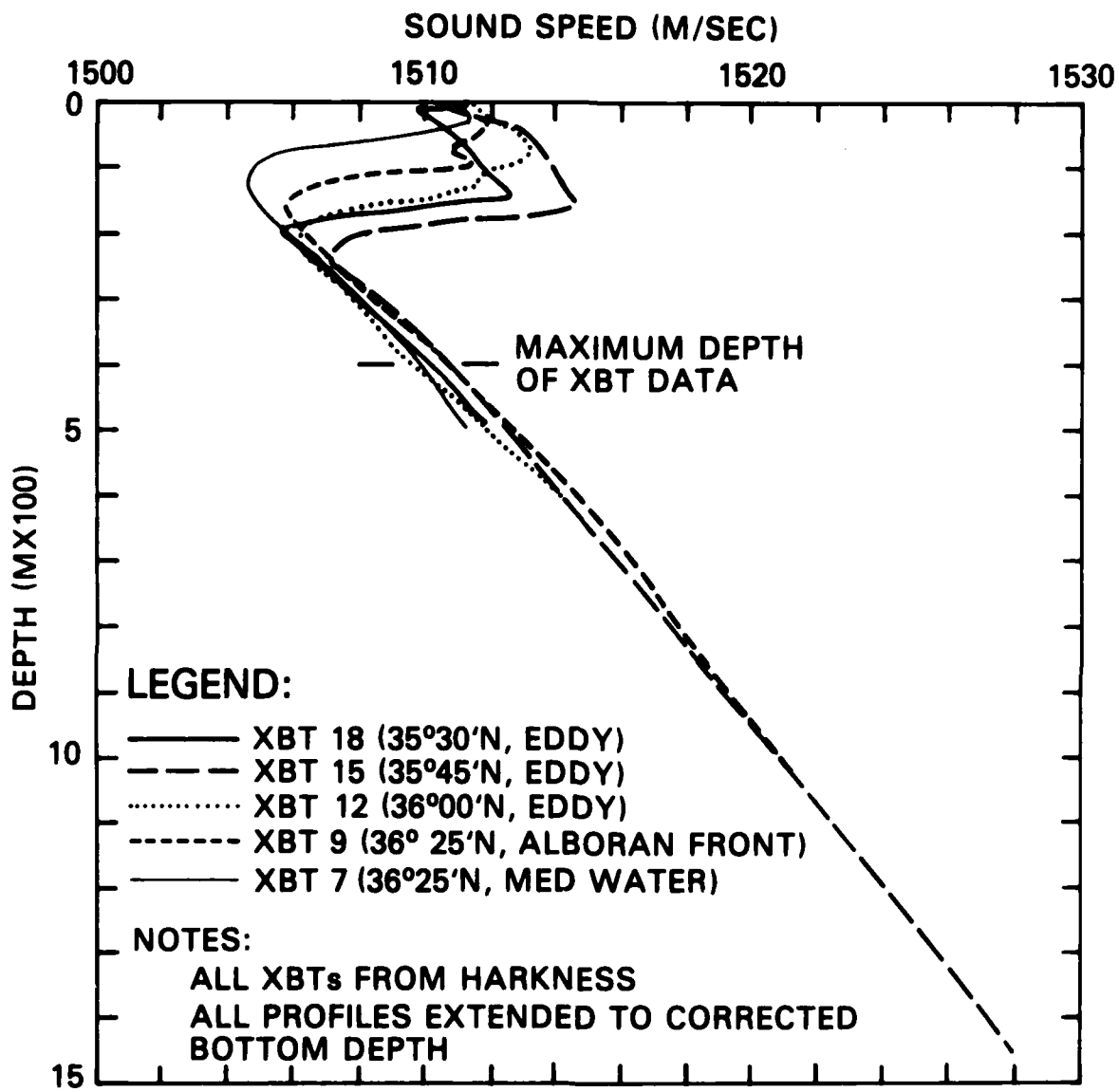


Figure 6. Sound speed composite along 1 February north-south track

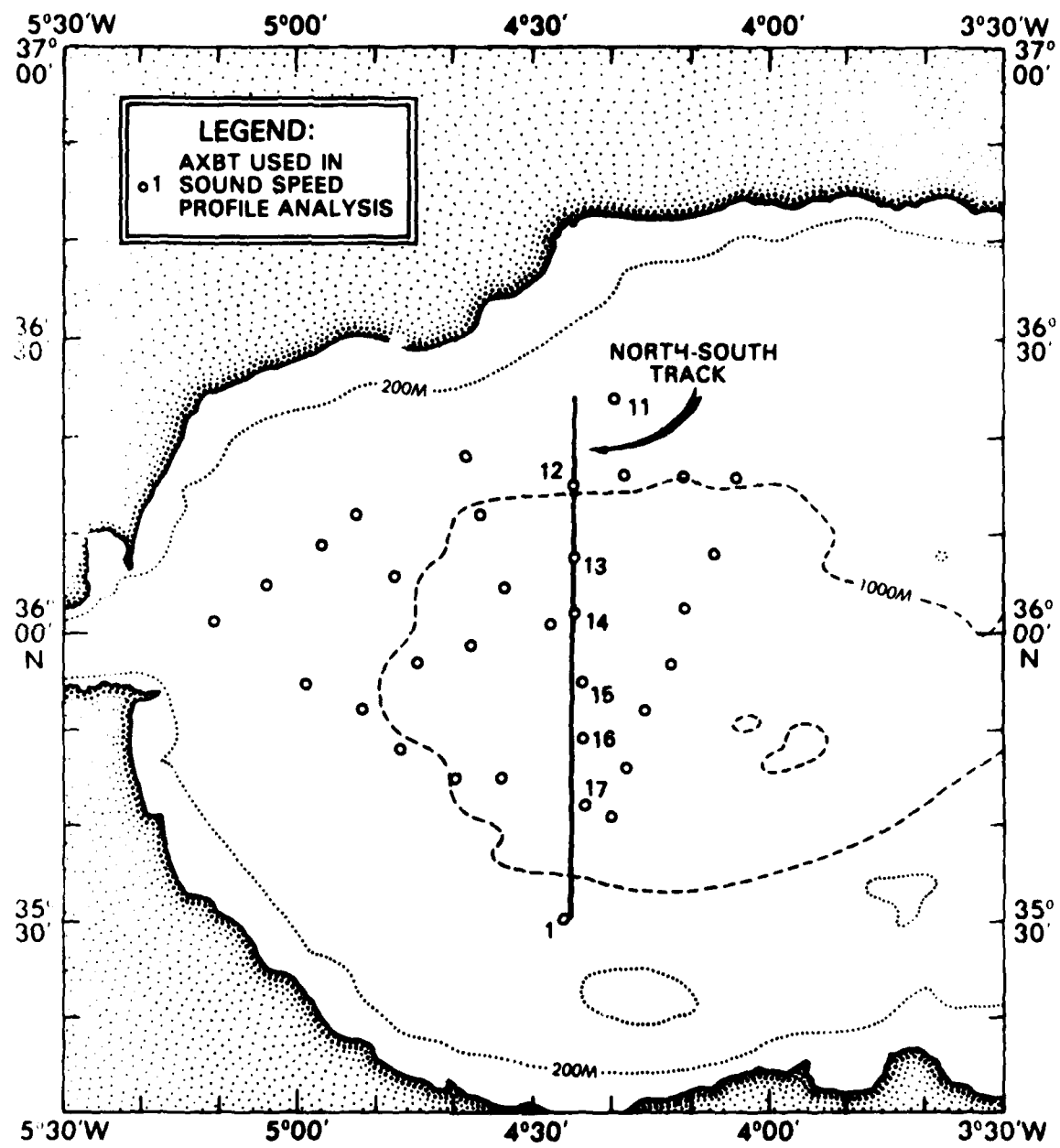


Figure 7. Location of 10 February AXBT data

meridional sound speed cross-section. Figure 8 shows contoured presentations of sea surface temperature, sonic layer depth, temperature at 100 m, and the depth of the deep sound channel axis based on all data collected on 10 February.

At the surface (Fig. 8a), the total temperature contrast was less than  $1.5^{\circ}\text{C}$  due to the effects of strong wind mixing (wind speeds up to 25 kn or 13 m/sec). However, the surface position of the Alboran Front was delineated by the  $17^{\circ}\text{C}$  isotherm. The  $17.5^{\circ}\text{C}$  surface isotherm apparently delineated the actual inflow of Atlantic Water, and indicated that incoming Atlantic Water may flow south along the African coast before becoming entrained in the anticyclonic gyre. At 100 m (Fig. 8c), the axis of the front corresponded to the  $15^{\circ}\text{C}$  isotherm. The width of the Alboran Frontal Zone varied from about 16 nm (30 km) along approximately  $40^{\circ}$  and  $50^{\circ}\text{W}$  to about 6 nm (11 km) along  $40^{\circ}30'W$ . The  $17^{\circ}\text{C}$  isotherm at 100 m depth apparently defined the core of inflowing Atlantic Water, again indicating that entrainment occurred along the African coast south of the Strait of Gibraltar. The position of the frontal axis at 100 m generally agreed with the surface position of the front, particularly along the northern edge of the anticyclonic gyre.

Sonic layer depth on 10 February (Fig. 8b) varied from greater than 180 m in the anticyclonic gyre to less than 20 m in the region north of about  $36^{\circ}\text{N}$ . The maximum gradient in sonic layer depth generally was centered about the 100 m isopleth, and occurred up to 10 nm (18 km) south of the position of the  $15^{\circ}\text{C}$  isotherm at 100 m depth. This situation is analogous to that found on 4 February. The convoluted form of the sonic layer depth isopleths for 10 February also is similar to that for 4 February (Fig. 4c), and indicates an injection of water from the north and west into the surface mixed layer. Such an injection would cause the formation of complex sound speed maxima and minima and could result in anomalously shallow sonic layer depths and multiple surface ducts. AXBT profiles 13 and 14 (see Fig. 10) show examples of complex mixed layer structures within and immediately south of the Alboran Frontal Zone. In the case of AXBT 13, the depth of the sonic layer occurred above the top of the thermocline. However, the top of the thermocline was marked by a sound speed maximum that was only slightly less than that maximum defined as sonic layer depth. In the case of AXBT 14, the depth of the sonic layer corresponded to the top of the thermocline. However, a sound speed maximum occurred above sonic layer depth that was only slightly lower than that defined as sonic layer depth. Both examples point out the highly variable nature of sonic layer depth, which can be altered by many physical phenomena, including surface isolation/cooling, wind mixing, and upwelling processes.

The depth of the deep sound channel axis on 10 February (Fig. 8d) varied from greater than 250 m near the center of the anticyclonic gyre to less than 100 m north of the Alboran Front. As was the case on 4 February (Fig. 4d), the 150 m and 200 m axial depth contours corresponded well with the position of the frontal zone.

Figure 9 shows a contoured sound speed cross-section along the 10 February north-south track. An overplot of selected sound speed profiles along the track is presented in Figure 10. At a depth of 100 m, the track intersected the Alboran Frontal Zone between about  $36^{\circ}08'$  and  $36^{\circ}13'N$  (i.e., between ranges of about 40 and 45 nm or 74 and 83 km, respectively). This intersection occurred at that point where the Alboran Frontal Zone was narrowest (Fig. 8c). As was the case along the 1 February meridional section (Fig. 5), the maximum gradient in sonic layer depth occurred south of the frontal zone. Between ranges of 32 and 38 nm (59 and 70 km), the sonic layer decreased in depth from 150 to 50 m (gradient of 16.7 m/nm or 9.1 m/km). The axis of the deep sound channel shoaled rapidly to the north within and just south of the Alboran Frontal Zone. Within the frontal zone, the axis rose from 200 m at 38 nm (70 km) to 110 m at 45 nm (83 km). The deep axial gradient

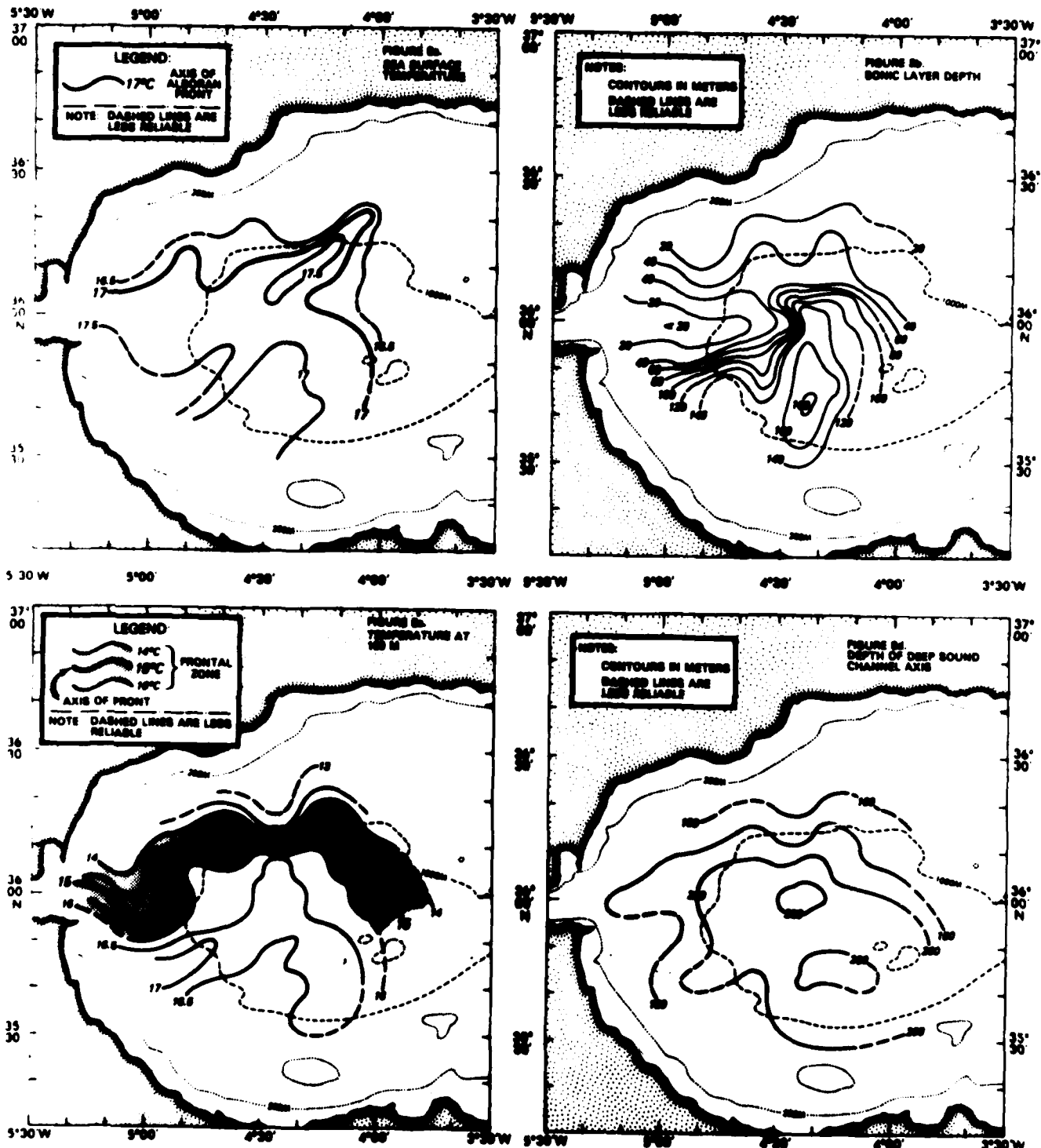


Figure 8. Temperature and sound speed parameters on 10 February

THIS PAGE IS BEST QUALITY PRACTICABLE  
DUKU COPY FURNISHED TO DDC

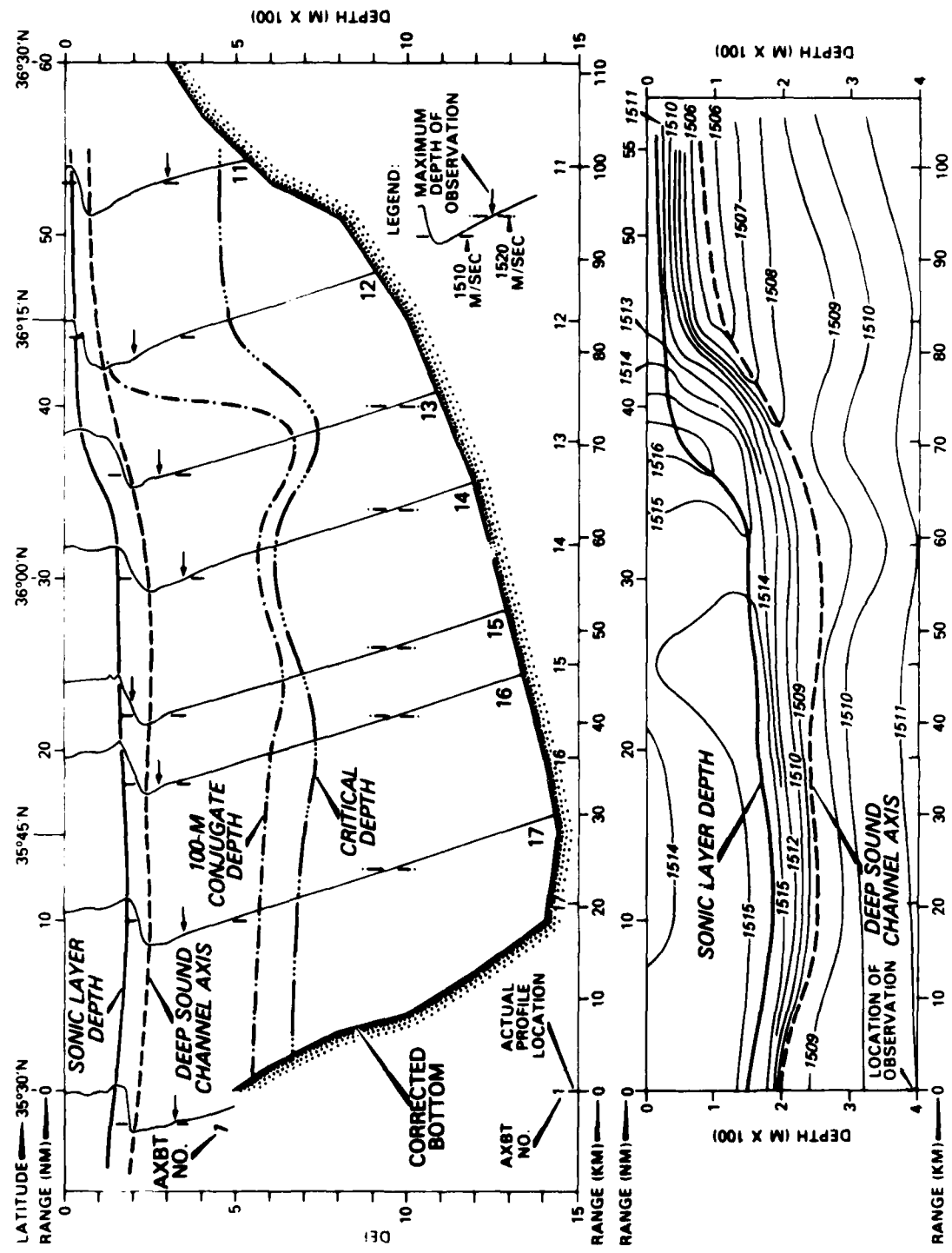


Figure 9. Sound speed cross section along 10 February north-south track

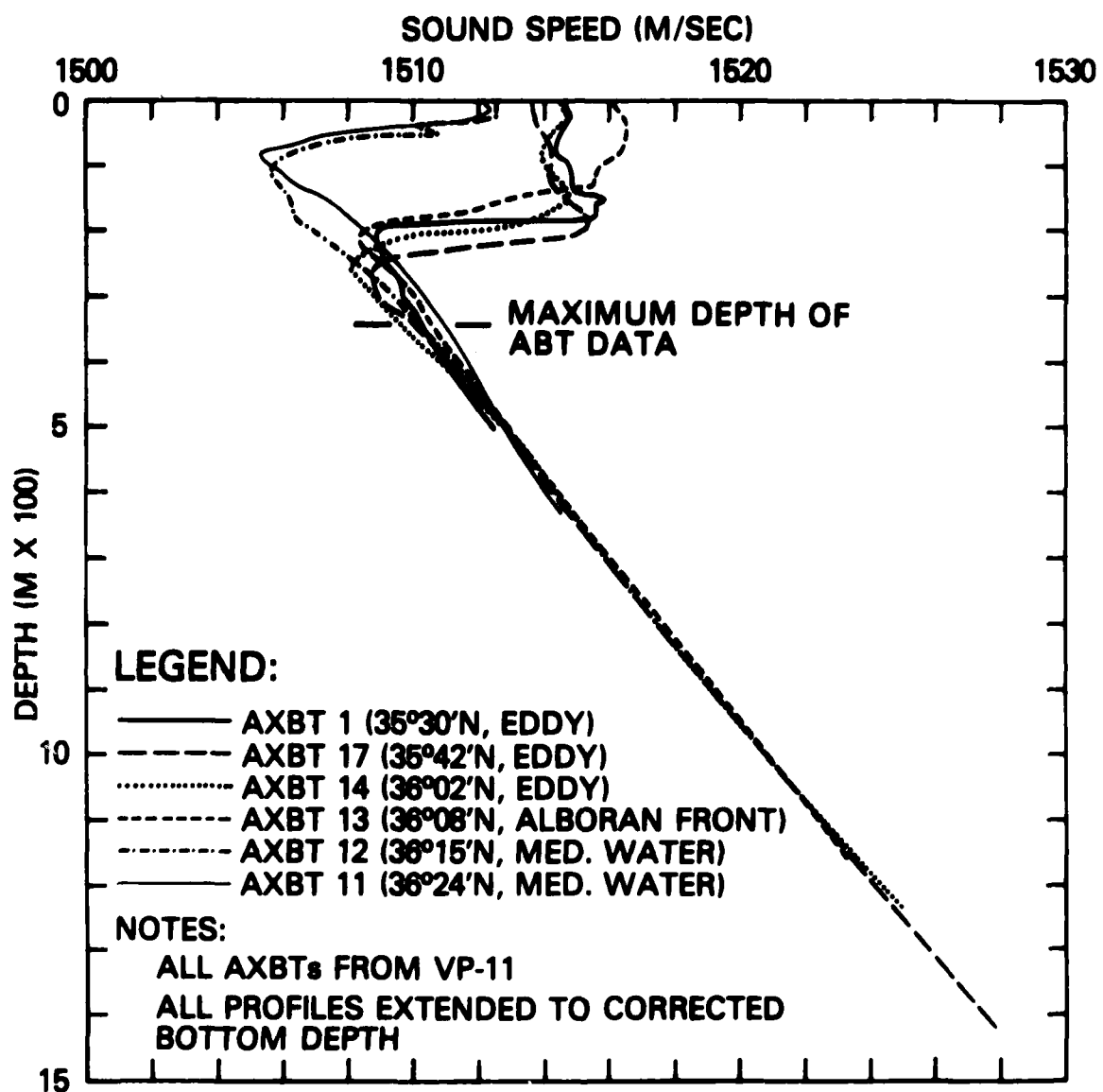


Figure 10. Sound speed composite along 10 February north-south track

across the frontal zone (12.9 m/nm or 6.9 m/km) was about one-third that found across the edge of a Gulf Stream anticyclonic eddy (Fenner, 1978). The bathymetry along the entire track was deeper than either critical or 100 m conjugate depth. Both these variables shoaled abruptly across the frontal zone, and 100 m conjugate depth effectively disappeared north of the frontal zone when the deep sound channel axis reached depths shallower than 100 m. However, depth excess along the entire meridional section was adequate to support convergence zone propagation from either a near-surface or 100 m source. The greatest spatial sound speed variability along the meridional section (about 11 m/sec) occurred at a depth of 75 m (Fig. 10).

#### VI. OCEANOGRAPHIC CONDITIONS ON 19 FEBRUARY

Figure 11 shows the location of AXBTs collected on 19 February by VP-11, and identifies those data used in the 19 February meridional sound speed cross-section. Figure 12 shows contoured presentations of sea surface temperature, sonic layer depth, temperature at 100 m, and the depth of the deep sound channel axis based on all data collected on 19 February.

At the surface (Fig. 12a), the Alboran Front was not discernable on 19 February. At a depth of 100 m (Fig. 12c), the Alboran Frontal Zone occupied approximately the same position as it had on 4 and 10 February. The width of the frontal zone varied from about 20 nm (37 km) along  $40^{\circ}15'W$  to about 3 nm (5 km) along  $40^{\circ}40'W$ . The frontal zone itself appeared more convoluted on 19 February than on the previous two sampling days. Sonic layer depths (Fig. 12b) varied from greater than 180 m within the gyre to 0 m (surface) north of the Alboran Front. The overall pattern of sonic layer depths on 19 February was noticeably more confused than on the previous two sampling days. However, unlike the cases for 4 and 10 February, anomalously shallow sonic layers were not generally present south of the frontal zone on 19 February. The depth of the deep sound channel axis (Fig. 12d) varied from 250 m within the gyre to less than 100 m north of the Alboran Front, and the 150 m deep axial depth contour approximated the axis of the front.

Figure 13 shows a contoured meridional sound speed cross-section for 19 February. An overplot of selected sound speed profiles along this section is presented in Figure 14. At a depth of 100 m, the section intersected the Alboran Frontal Zone between about  $36^{\circ}10'$  and  $36^{\circ}22'N$  (i.e., between ranges of 40 and 52 nm or 74 and 94 km, respectively). Both sonic layer depth and the depth of the deep sound channel axis shoaled abruptly across the frontal zone. The maximum gradient in sonic layer depth occurred within the frontal zone between ranges of 39 and 51 nm (72 and 93 km). Here, sonic layer depth decreased from 125 to 25 m (gradient of 8.3 m/nm or 4.8 m/km). The maximum gradient in deep axial depth along the section occurred south of the frontal zone between ranges of 28 and 33 nm (52 and 61 km). Here, deep axial depth decreased from 200 to 125 m at a gradient of 15.0 m/nm (8.3 m/km). This gradient is somewhat greater, but of the same general magnitude, as that observed within the frontal zone on 10 February (Fig. 9). Both critical and 100 m conjugate depth shoaled rapidly to the north across the frontal zone on 19 February. Depth excess, however, was more than adequate for convergence zone propagation from either a near-surface or 100 m source. The greatest sound speed variability (about 10 m/sec) along the section occurred at a depth of 150 m (Fig. 14).

#### VII. OCEANOGRAPHIC CONDITIONS ON 2-3 MARCH

Figure 15 shows the location of XBT and STD data taken by RESEARCHER on 2-3 March and identifies data used in the 2-3 March meridional sound speed cross-section (Fig. 16). Data from one STD station (STD 3 at the southern end of the

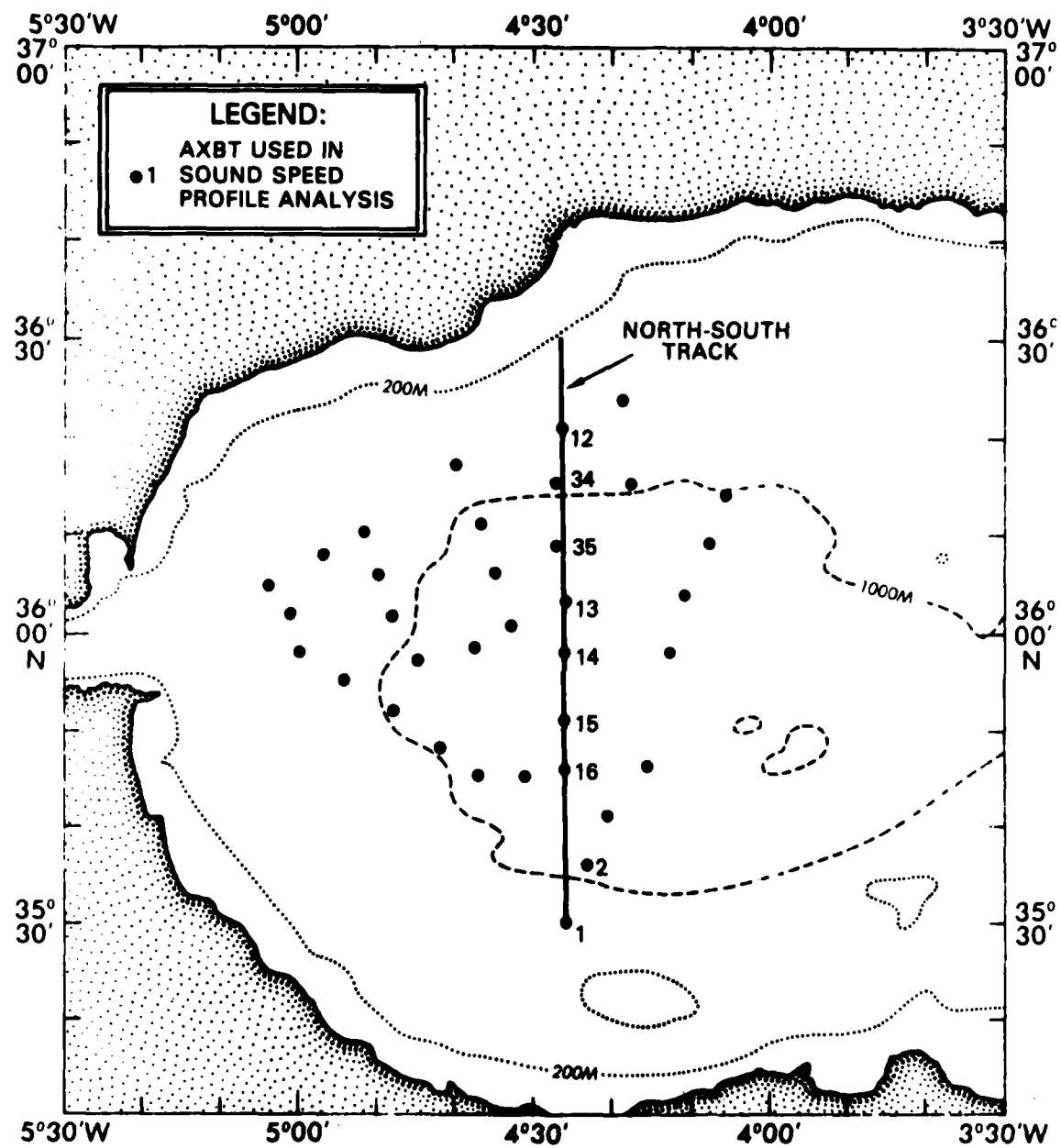


Figure 11. Location of 19 February AXBT data

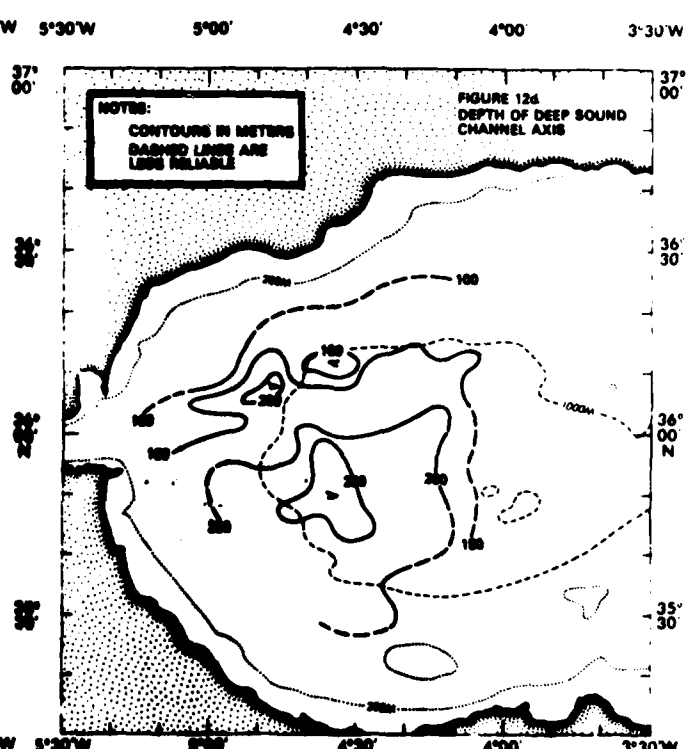
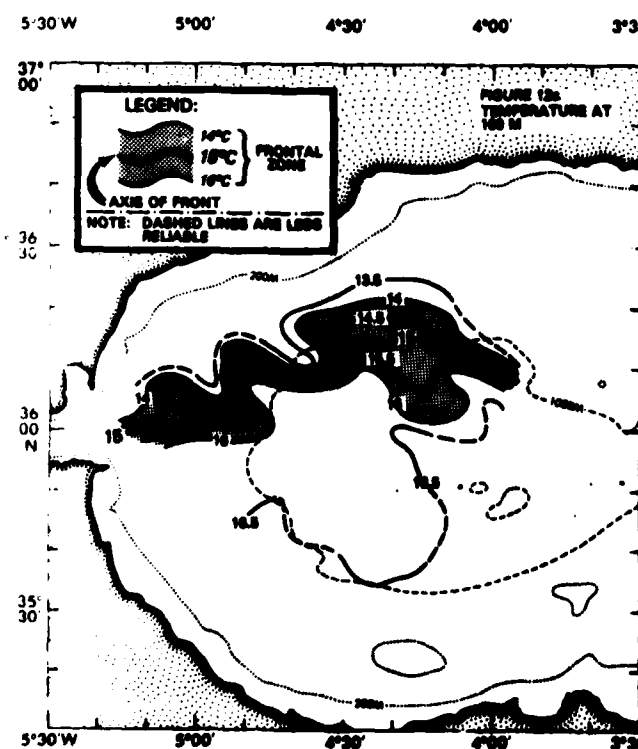
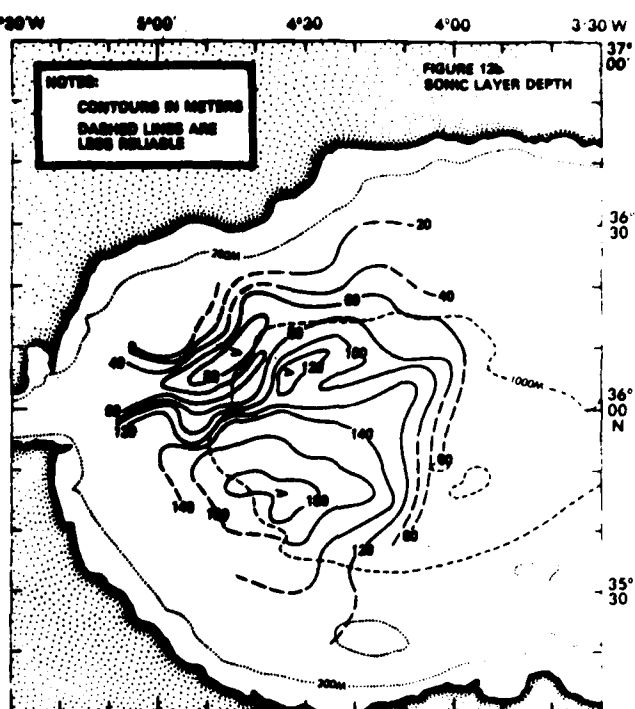
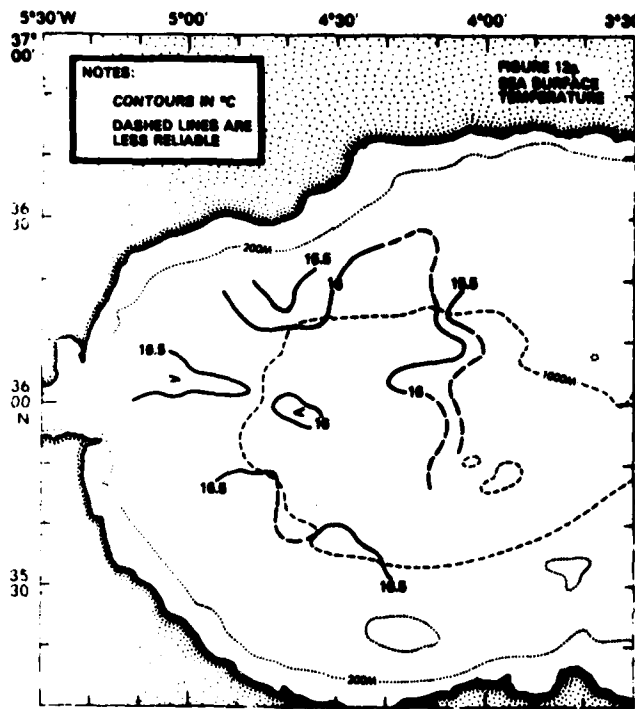


Figure 12. Temperature and sound speed parameters on 19 February

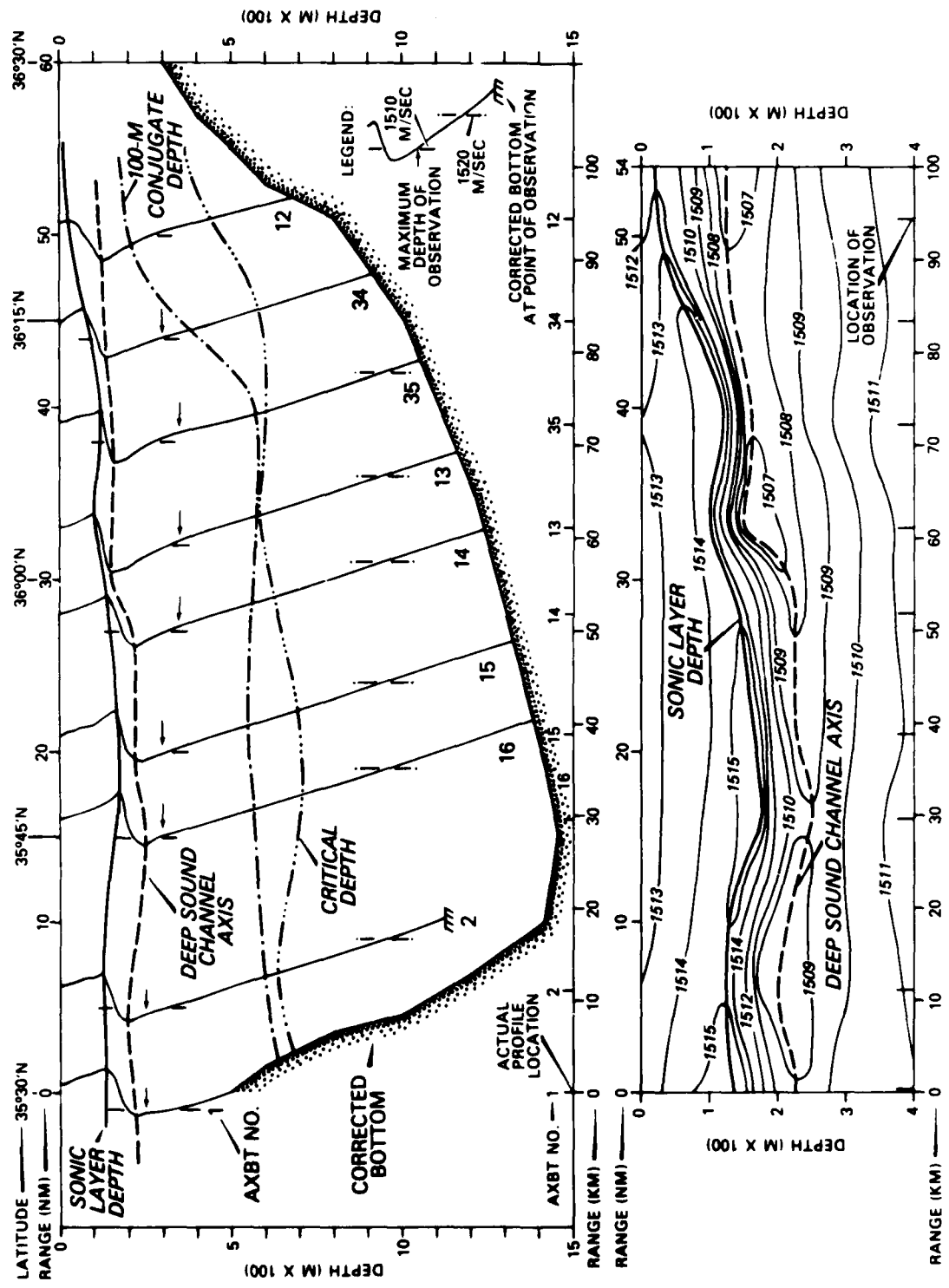


Figure 13. Sound speed cross section along 19 February north-south track

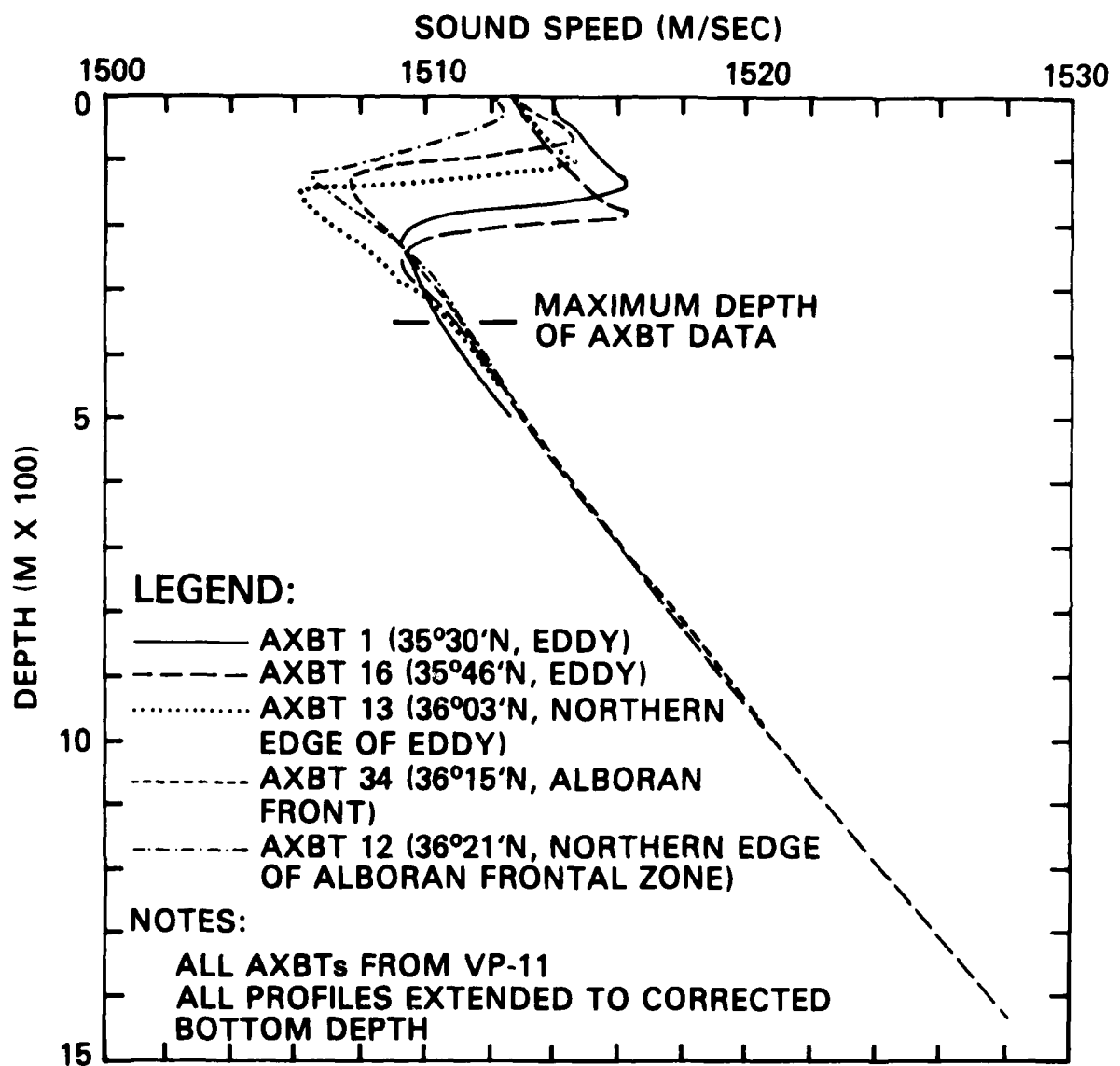


Figure 14. Sound speed composite along 19 February north-south track

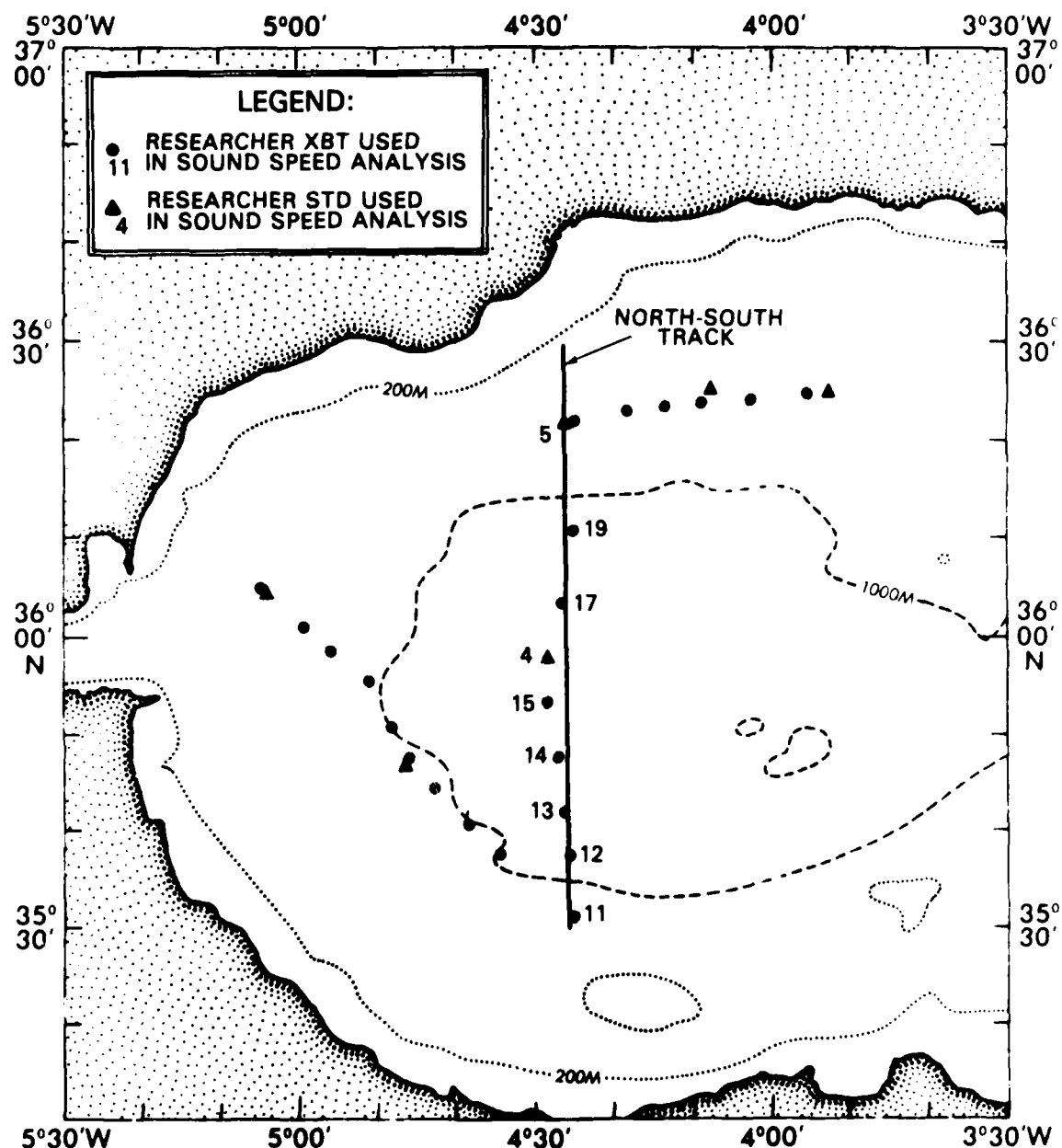


Figure 15. Location of 2-3 March STD/XBT data

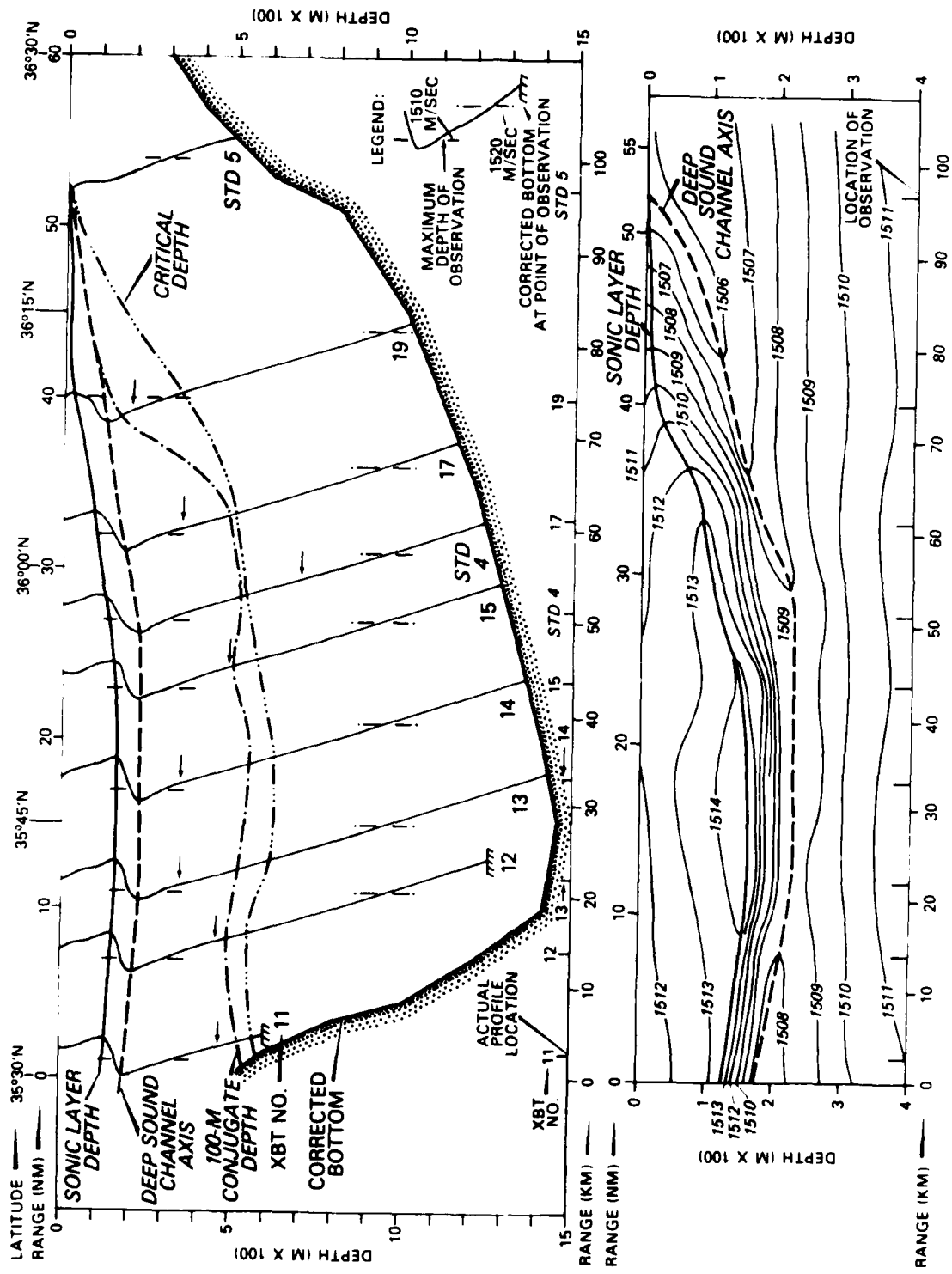


Figure 16. Sound speed cross section along 2-3 March north-south track

north-south track) was not usable due to data logger errors and extreme spikiness. However, data from the other two stations along the section (STDs 4 and 5) was usable. An overplot of selected sound speed profiles along the section is given in Figure 17.

The 2-3 March cross-section intersected the Alboran Frontal Zone between about  $36^{\circ}03'N$  and  $36^{\circ}10'N$  at ranges between about 33 and 40 nm (61 and 74 km). RESEARCHER XBT 17 showed a 100 m temperature of  $15.9^{\circ}C$ , placing it on the southern side of the frontal zone; XBT 19 had a 100 m temperature of  $14.0^{\circ}C$ , placing it on the northern edge of the frontal zone. Both sonic layer and deep axial depth shoaled markedly across the frontal zone. The maximum sonic layer depth gradient occurred within the frontal zone where the depth of the layer decreased from 90 to 20 m (gradient of 10.0 m/nm or 5.4 m/km). The maximum gradient in deep axial depth occurred north of the zone between ranges of 40 and 52 (74 and 96 km). Here, the depth of the axis decreased from 130 m to 0 m (surface) with a gradient of 10.8 m/nm (5.9 m/km). This gradient is weaker than, but of the same general magnitude as, that found south of the frontal zone on 10 February (Fig. 9) or within the frontal zone on 19 February (Fig. 13). Both critical and 100 m conjugate depths shoaled abruptly to the north across the frontal zone. Depth excess along the entire 2-3 March section was more than adequate for convergence zone propagation considering either near-surface or 100 m source. The greatest sound speed variability along the section as a whole (about 9 m/sec) occurred between depths of 140 and 160 m (Fig. 17).

#### VIII. SUMMARY OF TEMPORAL AND SPATIAL VARIABILITY ALONG NORTH-SOUTH TRACK

Figure 18 compares critical depth, sonic layer depth, and the depth of the deep sound channel axis along the north-south track (spatial variability) for the four days this track was occupied (temporal variability). This figure also shows the latitude extent of those samples considered in the sound speed time-series (Fig. 19). In both the temporal and spatial sense, critical depth remained relatively constant along the track on 1, 10, and 19 February and generally lay between 500 and 700 m. However, on 2-3 March, critical depth shoaled rapidly in the region north of about  $36^{\circ}N$  due to a more southerly position of the Alboran Front along the track. Sonic layer depth and the depth of the deep sound channel axis also displayed a great deal of temporal and spatial continuity, particularly south of  $36^{\circ}N$ . Here, the sonic layer generally occurred between depths of 100 and 175 m and deep axial depth generally lay at depths between 200 and 250 m. North of  $36^{\circ}N$ , sonic layer and deep axial depth were more variable both temporally and spatially due to changes of position and meandering of the Alboran Front. Generally, sound speed conditions were remarkably stable along the meridional section over the course of the exercise (4-19 February) and throughout the month of February 1979.

#### IX. TEMPORAL VARIABILITY IN SOUND SPEED AT $36^{\circ}00'N$ , $4^{\circ}28'W$

Figure 19 shows a composite of sound speed profiles collected within 6 nm (11 km) of  $36^{\circ}00'N$ ,  $4^{\circ}28'W$ , near the center of the north-south track. The profiles were collected between 26 January and 19 March, and include both XBT and AXBT data. Several temperature and sound speed parameters for each profile (temperature at 100 and 300 m, sonic layer depth, and the depth and sound speed at the deep sound channel axis) are listed in a table accompanying Figure 19. As previously mentioned, XBTs measure temperature to about  $\pm 0.2^{\circ}C$ , and yield calculated sound speeds accurate to about  $\pm 0.8$  m/sec. Comparable accuracy figures for the AN/SSQ-36 AXBT are about  $\pm 0.3^{\circ}C$  and  $\pm 1.3$  m/sec.

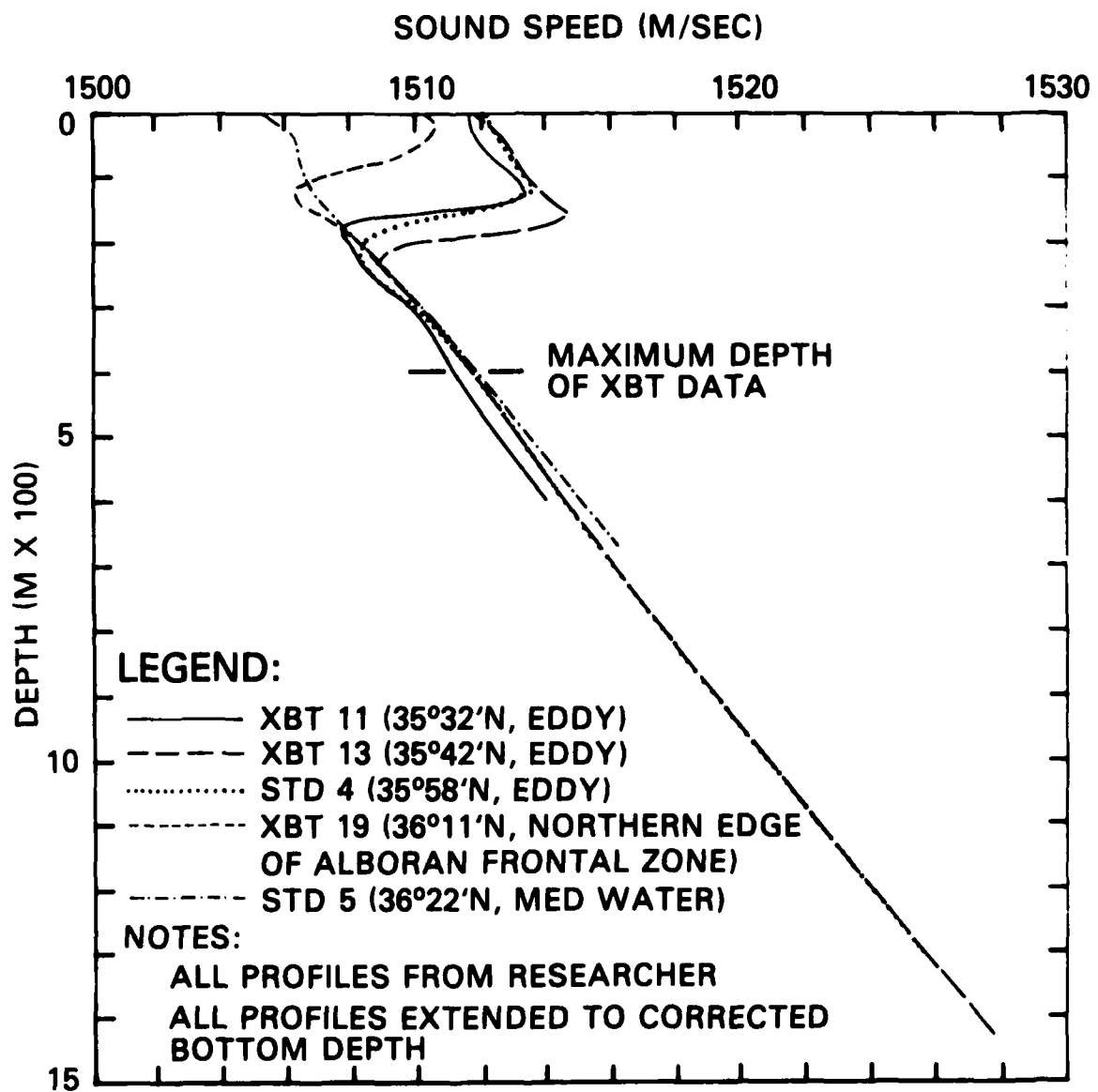


Figure 17. Sound speed composite along 2-3 March north-south track

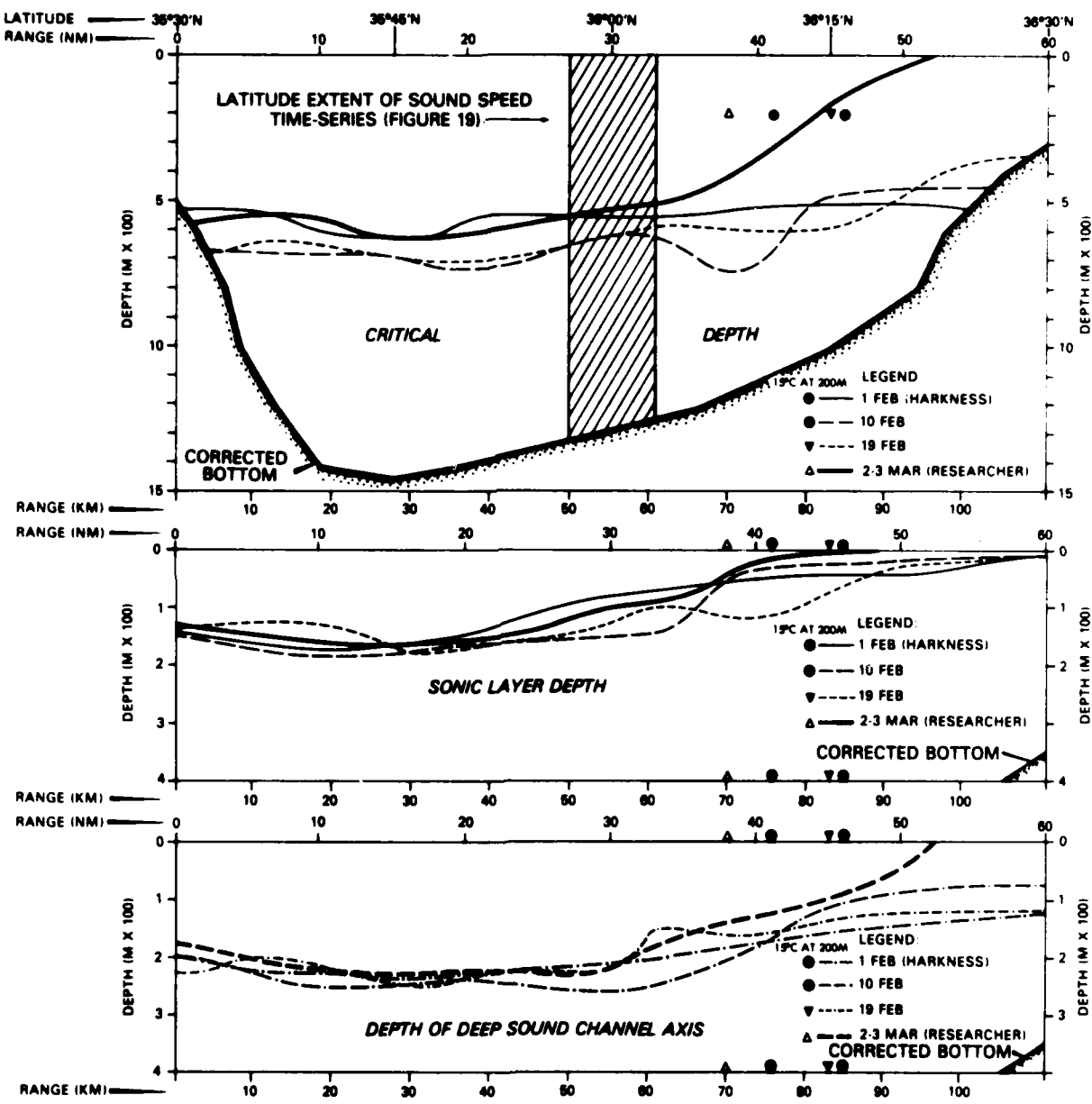
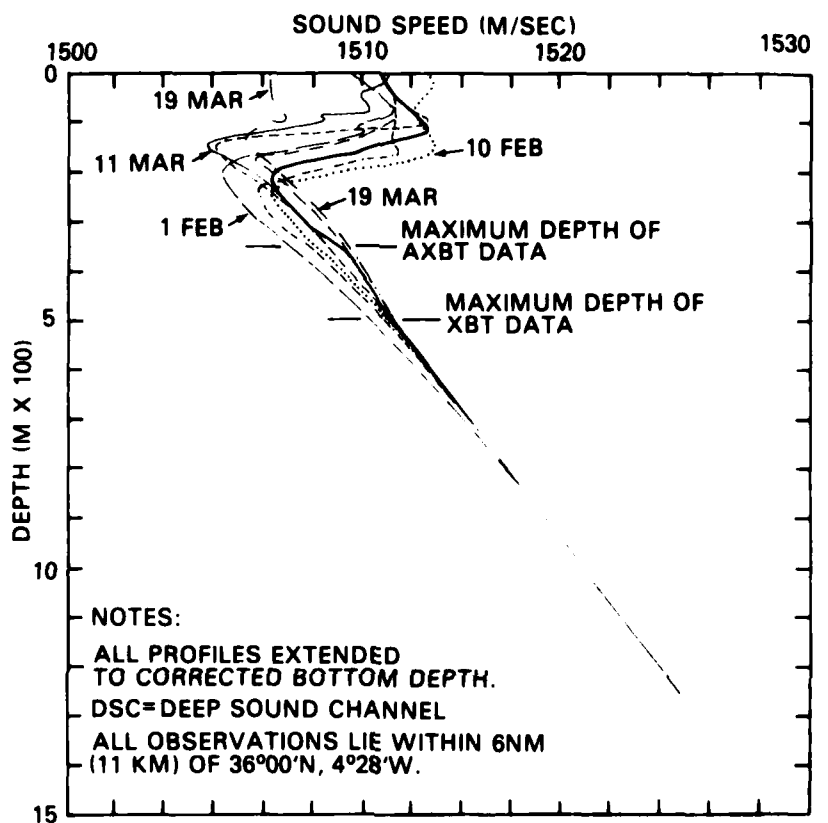


Figure 18. Comparison of sound speed parameters along north-south track



#### LEGEND:

- VZN-8 AXBT 58 (26 JAN)
- - HARKNESS XBT 12 (01 FEB)
- - VP-11 AXBT 16 (04 FEB)
- - VP-11 AXBT 14 (10 FEB)
- - VP-11 AXBT 13 (19 FEB)
- - RESEARCHER XBT 17 (03 MAR)
- - VZN-8 AXBT 4 (11 MAR)
- - VZN-8 AXBT 1 (19 MAR)

TEMPERATURE AT 100M (°C)	TEMPERATURE AT 300M (°C)	SONIC LAYER DEPTH (M)	DEPTH OF DSC AXIS (M)	SOUND SPEED AT DSC AXIS (M/SEC)
16.3	13.2	120	210	1508.1
15.7	12.6	80	210	1506.2
16.0	12.8	160	240	1507.5
16.5	13.0	150	250	1508.1
16.4	13.2	100	150	1506.0
15.9	13.3	90	180	1507.5
15.8	13.2	0	150	1505.6
14.2	13.4	100	135	1507.2

Figure 19. Temporal variability in sound speed near center of north-south track

The time-series site lay within the warm anticyclonic gyre throughout most of the sampling period (temperature at 100 m greater than 15°C). Even on 11 March (VXN-8 AXBT 4), when the Alboran Front was approaching the site (Fig. 20), the temperature at 100 m was 15.8°C. However, by 19 March (VXN-8 AXBT 1) the temperature at 100 m had decreased to 14.2°C, indicating that the time-series site lay in colder Mediterranean Water rather than within the anticyclonic gyre. Sonic layer depth at the site varied from a maximum of 160 m on 4 February (typical of conditions within the gyre) to a minimum of 0 m (surface) on 11 March (when Alboran Front was approaching the site). The depth of the deep sound channel axis varied from 250 m on 10 February, conditions typical of the gyre, to 135 m on 19 March when the site lay in colder Mediterranean Water. The sound speed at the deep sound channel axis varied from 1508.1 m/sec on 10 February, conditions typical of the gyre, to 1505.6 m/sec on 11 March, a condition typical for colder Mediterranean Water.

Below a depth of about 300 m, sound speed values on 1 February (HARKNESS XBT 12) and 4 February (VP-11 AXBT 16) were generally lower than those found on other sampling days. This is directly related to generally lower temperatures throughout the water column on both days. At 300 m, the temperature was 12.6°C on 1 February and 12.8°C on 4 February. Both values are less than those expected on the basis of historical data from the western Alboran Sea (13.0  $\pm$  0.2°C). However, considering instrumentation accuracy, the HARKNESS XBT temperature at 300 m could be as high as 12.8°C, and the VP-11 AXBT temperature could be as high as 13.1°C, both within the range of the historical data. In any case, the HARKNESS XBT observations collected on 1 February and the VP-11 AXBTs collected on 4 February are considered to be an accurate measurement of environmental conditions on these two days. Other investigators also have found "deep" temperatures lower than 13.0  $\pm$  0.2°C in the western Alboran Sea, including during the recent HUELVA Exercise (J. Gallagher, NUSC/NL, personal communication, August 1979).

Between 26 January and 19 March, maximum temporal variability in sound speed at the time-series site (about 11 m/sec) occurred at a depth of 125 m. The magnitude of temporal variability near the center of the north-south track is similar to the magnitude of spatial variability encountered along the track as a whole on each of the four days the track was occupied (i.e., 10 m/sec on 1 February, 11 m/sec on 10 February, 10 m/sec on 19 February, and 9 m/sec on 2-3 March). The depth of maximum sound speed variability at the time-series site (125 m) lay between the various depths of maximum spatial variability along the entire meridional section (i.e., 75 m on 10 February and 140-160 m on 1 February, 19 February, and 2-3 March). The similar magnitude and depth of temporal and spatial variability indicate that these variabilities are caused by similar natural phenomena. Suspected phenomena include air-sea interactive processes, frontal meandering, and injection of colder water from the north into the surface mixed layer of the anticyclonic gyre.

#### X. TEMPORAL VARIABILITY OF THE ALBORAN FRONT AND ANTICYCLONIC GYRE

Figure 20 shows the position of the Alboran Front axis (15°C isotherm at a depth of 100 m) for seven selected days, including three days (4, 10, and 19 February) within the time frame of the exercise. Between 26 January and 19 February, the axis of the front lay in basically the same position along the 1000 m bathymetric contour, but displayed extensive meandering. However, by 2-3 March, the Alboran Front axis had moved 5-10 nm (9-18 km) south of its average position during the exercise, and by 10-11 March, the anticyclonic gyre was absent in the region west of about 40°30'W. Even during the exercise time frame, when the position of the Alboran Front axis was relatively stable, the anticyclonic eddy of warmer Atlantic

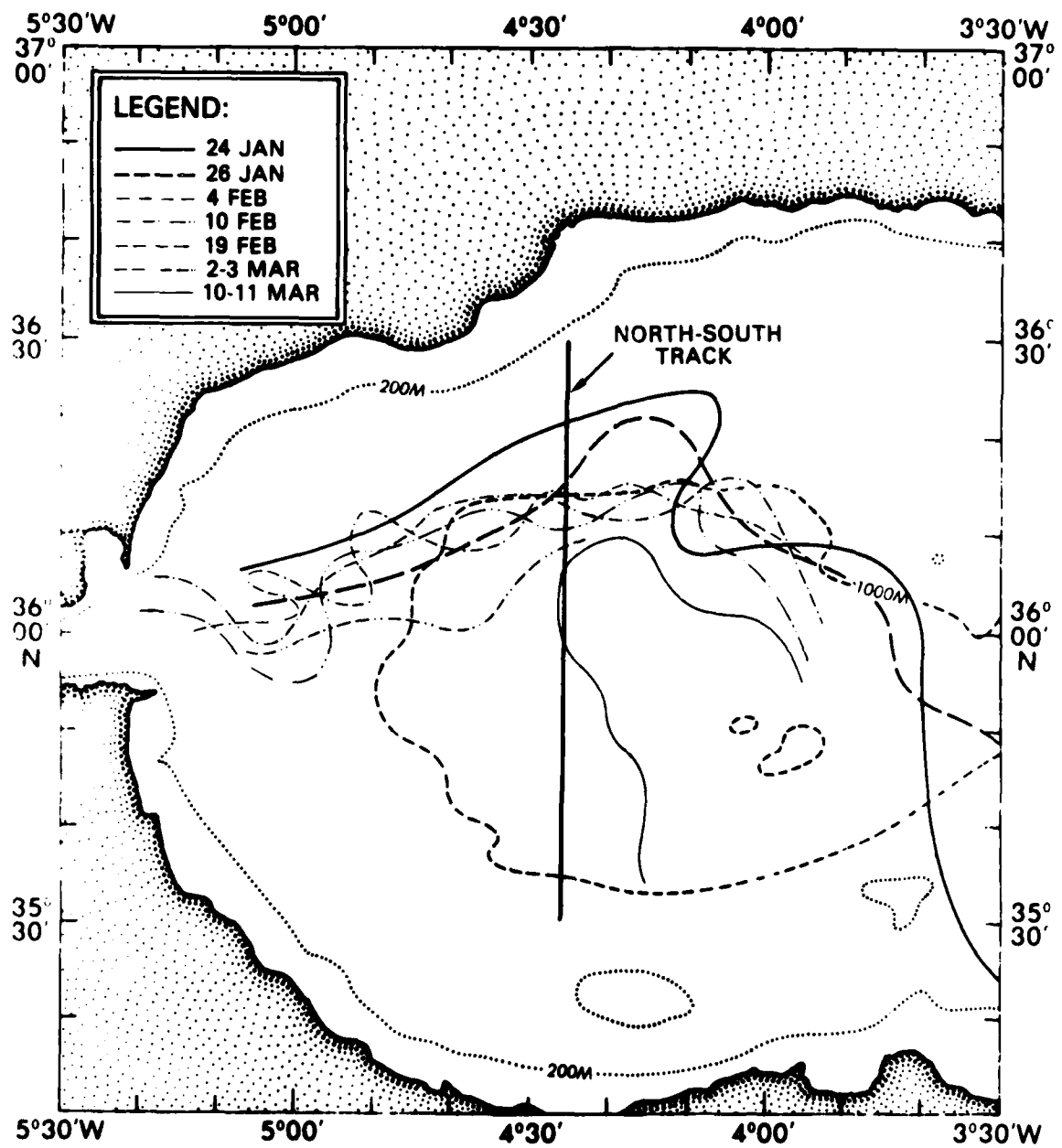


Figure 20. Mean position of Alboran Front at 100 m (24 January-22 March 1979)

Water underwent changes in position and intensity, mainly as a result of atmospheric forcing.

According to Crepon (1965), and as substantiated by Cheney and Doblar (1975), atmospheric pressure over the western Mediterranean plays an important role in determining the rate of Atlantic Water inflow through the Strait of Gibraltar. In the presence of an atmospheric high pressure cell over the western Mediterranean, the sea surface becomes depressed, tending to force water out through the Strait. This results in minimal inflow, and in a smaller anticyclonic gyre located in a more westerly position. However, during the passage of an atmospheric low pressure system over the Mediterranean, the sea surface rises, drawing more Atlantic Water through the Strait. This results in a larger anticyclonic eddy located in a more easterly position. In the case of a cold front passage over the Alboran Sea, the local wind stress and pressure act together to increase the inflow of Atlantic Water. Average transport through the Strait of Gibraltar can easily double under these conditions (Lacombe and Tcherina, 1971).

On 4 February, atmospheric pressure over the western Mediterranean Sea was relatively high (greater than 1016 mb) according to the Weather Log of the Royal Meteorological Society (1979a). This should have somewhat restricted the flow of Atlantic Water through the Strait of Gibraltar and resulted in a somewhat reduced anticyclonic eddy located in the western portion of the exercise area. This situation is borne out by patterns of sea surface temperature, sonic layer depth, and deep axial depth for 4 February (Fig. 4). Based on deep axial depth contours (Fig. 4d), the gyre was centered at about  $35^{\circ}37'N$ ,  $40^{\circ}28'W$  on 4 February.

On 10 February, a cold front passed over the western Alboran Sea and atmospheric pressure dropped to about 1004 mb. Frontal passage was accompanied by winds up to 25 kn (13 m/sec) from the west and northwest. This apparently resulted in increased Atlantic Water inflow through the Strait of Gibraltar that also caused the Alboran Front to be discernable in sea surface temperature patterns (Fig. 8a). A strong flow of water from the west is discernable in sonic layer depth patterns (Fig. 8b) and in the patterns of temperature at 100 m (Fig. 8c). However, the position of the Alboran Front along the northern boundary of the gyre on 10 February was basically the same as that on 4 February. Based on deep axial depth contours (Fig. 8d), the gyre was centered at about  $35^{\circ}42'N$ ,  $40^{\circ}10'W$  on 10 February, about 8 nm (15 km) east of its position on 4 February.

By 19 February, atmospheric pressure was again greater than 1016 mb over the western Mediterranean. Contour patterns for sea surface temperature, sonic layer depth, and deep axial depth for 19 February (Fig. 12) show that the eddy was again confined to the western part of the exercise area (west of about  $40^{\circ}10'W$ ). Based on deep axial depth contours (Fig. 12d), the gyre was centered at about  $35^{\circ}50'N$ ,  $40^{\circ}35'W$ . This position is 20 nm (37 km) west of the apparent eddy center on 10 February and even somewhat west of the apparent eddy center on 4 February. However, the position of the Alboran Front axis was basically the same on 19 February as it was on 4 and 10 February.

On 2-3 March, atmospheric pressure over the western Alboran Sea reached 1032 mb (Royal Meteorological Society, 1979b), caused by a high pressure cell centered just west of the Strait of Gibraltar. This high pressure cell should have severely restricted the inflow of Atlantic Water through the Strait, and may have been responsible for the pronounced southward shift of the Alboran Front axis observed on 2-3 March. Between 4 and 11 March, atmospheric pressure over the western Mediterranean consistently was greater than 1024 mb, and probably continued to restrict Atlantic Water inflow. However, unless inflow was effectively blocked (an

unlikely case), atmospheric forcing alone could not have been responsible for the disappearance of the warm, anticyclonic gyre from the region west of  $40^{\circ}30'W$  that was observed on 10-11 March. Other possible causes for this disappearance might include intensive cooling of the sea surface followed by convective mixing, intensive upwelling along the northern edge of the Alboran Sea followed by a flow of upwelled water to the south and east, or a combination of both.

## XI. SUMMARY

Between 24 January and 19 March 1979, a total of 183 AXBTs, 48 T-4 XBTs, and 6 STDs were taken in the western Alboran Sea (west of about  $30^{\circ}30'W$ ) in support of a Fleet-oriented exercise. Data collection support was provided by two Naval Aircraft Squadrons, the Naval Oceanographic Office, and the National Oceanic and Atmospheric Administration. All oceanographic data were converted to sound speed using the equation of Mackenzie (1976 and 1977) and either historical or in situ salinities. The overall distribution of oceanographic data was more than adequate to define environmental effects on acoustic propagation over the course of the exercise.

One of the most pronounced fronts in the Mediterranean occurs in the western Alboran Sea. The Alboran Front separates an anticyclonic gyre of warm, lower salinity Atlantic Water emanating through the Strait of Gibraltar from cooler, higher salinity Mediterranean Water. The Alboran Frontal Zone is generally confined to the upper 200-250 m of the water column and has a horizontal temperature gradient of  $\sim 4^{\circ}C$ . During winter, the axis or mean position of the front corresponds to the  $17^{\circ}C$  isotherm at the surface and the  $15^{\circ}C$  isotherm at a depth of 100 m. During winter, sonic layer depth in the western Alboran Sea corresponds to the maximum depth of winter cooling, while the deep sound channel axis coincides with the bottom of the permanent thermocline and generally defines the bottom of the warm, anticyclonic eddy.

Oceanographic data from 4, 10, and 19 February were analyzed on an areal basis in terms of sea surface temperature, sonic layer depth, temperature at 100 m, and the depth of the deep sound channel axis. The Alboran Front was discernable at the surface only on 10 February. At a depth of 100 m, the axis of the Alboran Front ( $15^{\circ}C$  isotherm) was found across the western Alboran Sea on all three days between latitudes of about  $36^{\circ}10'$  and  $36^{\circ}20'N$ . Despite considerable meandering, the frontal axis generally followed the 1000 m bathymetric contour east of about  $40^{\circ}50'W$ . Frontal zone width (i.e., the distance between the  $14^{\circ}C$  and  $16^{\circ}C$  isotherms at 100 m measured normal to the frontal axis) varied from about 3 nm (6 km) to about 20 nm (37 km). Sonic layer depths varied from greater than 180 m in the center of the gyre to less than 20 m in the region north of the Alboran Front on all three days. On 4 and 10 February, maximum sonic layer depth gradients occurred south of the Alboran Frontal Zone rather than within the frontal zone. This may have been caused by an injection of colder, upwelled water from the north into the surface mixed layer. On all three days, the depth of the deep sound channel axis varied from greater than 250 m within the gyre to 100-150 m north of the front. Generally, the 150 and 200 m axial depth isopleths described the width of the Alboran Frontal Zone.

Meridional sound speed cross-sections along about  $40^{\circ}30'W$  were constructed for 1, 10, and 19 February and for 2-3 March. Sound speed conditions were remarkably stable along  $40^{\circ}30'W$  during all four periods. The bathymetry along the cross-section was considerably deeper than either critical or 100 m conjugate depth, providing more than enough depth excess for convergence zone propagation from either a near-surface or a 100 m source. Sonic layer and deep axial depth shoaled abruptly either across or immediately south of the Alboran Frontal Zone during all four periods. A maximum horizontal gradient in sonic layer depth of  $1.7 \text{ m/nm}$  ( $9.1 \text{ m/km}$ )

was observed just south of the frontal zone on 1 February. A maximum horizontal gradient in deep axial depth of 15.0 m/nm (8.3 m/km) occurred on 19 February, also immediately south of the frontal zone. The maximum deep axial gradient was only about one-third the magnitude of that observed across the edge of a Gulf Stream anticyclonic eddy (Fenner, 1978), but probably is the greatest such gradient encountered in the Mediterranean Sea.

Sound speed profiles collected near the center of the meridional cross-section (within 6 nm (11 km) of 36°00'N, 4°028'W) were analyzed temporally over the course of the exercise. Between 26 January and 19 March, sonic layer depth varied by 160 m, deep axial depth by 115 m, and deep axial sound speed by 2.5 m/sec. Maximum temporal variability in sound speed (about 11 m/sec) occurred at a depth of 125 m. The magnitude and depth of maximum temporal variability near the center of the meridional section were similar to the magnitude and depth of spatial variability over the whole section on the four days the track was occupied. This indicates that temporal and spatial sound speed variability in the western Alboran Sea were caused by similar natural phenomena. Suspected phenomena include air-sea interactive processes, meandering of the Alboran Front, and injection of colder, upwelled water from the north into the surface mixed layer of the anticyclonic gyre.

As originally shown by Crepon (1965) and more recently by Cheney and Doblar (1979), atmospheric forcing can play an important role in determining Atlantic Water inflow through the Strait of Gibraltar, and hence on the size and position of the Alboran Sea anticyclonic gyre. Results from the exercise substantiated these previous findings. On 4 February, atmospheric pressure over the western Mediterranean was relatively high (greater than 1016 mb) and probably restricted Atlantic Water inflow. This resulted in a somewhat reduced anticyclonic gyre located generally west of 4°20'W. On 10 February, the passage of an atmospheric cold front over the Alboran Sea reduced pressures to less than 1004 mb, and apparently resulted in increased inflow through the Strait. In response, the anticyclonic gyre increased in size and was centered about 8 nm (15 km) east of its 4 February position. Higher atmospheric pressure on 19 February (greater than 1016 mb) resulted in a reduced gyre centered 20 nm (37 km) west of its apparent position on 10 February. None of the above atmospheric events significantly changed the position of the Alboran Front axis along the northern edge of the gyre. However, by 2-3 March the position of the Alboran Front axis had shifted 5-10 nm (9-18 km) south of its overall position during the exercise, and by 10-11 March the gyre was absent from the region west of about 4°30'W (meridional section). The pronounced southward shift of the Alboran Front axis on 2-3 March may have been caused by a high pressure cell off Gibraltar (1032 mb). However, the disappearance of the gyre from west of 4°30'W by 10-11 March probably was not totally caused by atmospheric forcing.

XII. REFERENCES

Bryden, H.L., R.C. Millard, and D.L. Porter (1978). CTD Observations in the Western Mediterranean Sea During Cruise 118, Leg 2 of R/V CHAIN, February, 1975. Woods Hole Oceanographic Institution, Woods Hole, Mass. (WHOI Rep. 78-26), 38 p.

Cheney, R.E. (1977). Recent Observations of the Alboran Sea Front. Naval Oceanographic Office, Washington, D.C., NAVOCEANO Tech. Note 3700-73-77, 22 p.

Cheney, R.E. (1978). Recent Observations of the Alboran Sea Frontal System. J. Geophys. Res., v. 83, n. C9, p. 4593-4597.

Cheney, R.E. and R.A. Doblar (1979). Alboran Sea 1977: Physical Characteristics and Atmospherically Induced Variations of the Oceanic Frontal System. Naval Oceanographic Office, NSTL Station, Miss., NAVOCEANO Tech Note 3700-82-79, 24 p.

Crepon, M. (1965). Influence of Atmospheric Pressure on the Mean Sea Level of the Western Mediterranean and on the Transport through the Strait of Gibraltar. Cashiers Oceanographique, v. 17, n. 1, p. 15-32 (in French).

Fenner, D.F. (1978). Sound Speed Structure Across an Anticyclonic Eddy and the Gulf Stream North Wall. J. Geophys. Res., v. 83, n. C9, p. 4599-4605.

Lanoix, F. (1972). Hydrological and Dynamic Study of the Alboran Sea. North Atlantic Treaty Organization, Brussels, NATO Tech. Rep. 66 (in French).

Lacombe, H. and D. Tcherina (1971). Hydrological Characteristics and Water Circulation in the Mediterranean. In: The Mediterranean Sea: A Natural Sedimentation Laboratory (D.J. Stanley, ed.). Dowden, Hutchison, and Ross, Inc., Stroudsburg, Penn., 765 p.

Mackenzie, K.V. (1976). Sound Speed in the Oceans. Presented at Joint Oceanographic Assembly, Edinburgh, September.

Mackenzie, K.V. (1977). Effects of Sound-Speed Equations on Critical Depths in the Oceans. Presented at 94th Meeting of the Acoustical Society of America, Miami Beach, Fla., December.

Ovchinnikov, I.M., V.K. Krivosheya, and L.V. Maskalenko (1976). Anomalous Features of the Water Circulation of the Alboran Sea During the Summer of 1962. Oceanology, v. 15, n. 1, p. 31-35 (translated from Russian by Amer. Geophys. Union).

Royal Meteorological Society (1979a). Weather Log, February 1979. Weather, v. 34, n. 4, April, unnumbered insert.

Royal Meteorological Society (1979b). Weather log, March 1979. Weather, v. 34, n. 5, May, unnumbered insert.

Wust, G. (1961). On the Vertical Circulation of the Mediterranean Sea. J. Geophys. Res., v. 66, n. 10, October, p. 3261-3271.

DISTRIBUTION LIST

Commander  
Sixth Fleet  
FPO New York, NY 09501 (1)

Commander Fleet Air, Mediterranean  
Commander, Antisubmarine War Force  
U. S. Sixth Fleet  
FPO New York, NY 09521 (1)

Commanding Officer  
Naval Oceanography Command Center  
Box 31  
FPO New York, NY 09540 (1)

Commander-In-Chief  
U. S. Naval Forces, Europe  
FPO New York, NY 09501 (1)

Commander  
Task Force 60  
FPO New York, NY 09501 (1)

Commander  
Task Force 67  
FPO New York, NY 09501 (1)

Commander  
Task Force 69  
Box 16  
FPO New York, NY 09501 (1)

Officer in Charge  
New London Laboratory  
Naval Underwater Systems Center  
New London, CT 06320  
Attn: Code 31 (1)  
Code 311 (1)  
Code 311M (1)  
Code 312 (Mr. Dullea) (1)  
Code 312 (Mr. Schumacher) (1)

Officer in Charge  
Newport Laboratory  
Naval Underwater Systems Center  
Newport, RI 02840  
Attn: Code 311 (1)  
Code 311 (Dr. Connors) (1)

Commander  
Naval Ocean Systems Center  
San Diego, CA 92152  
Attn: Code 5301 (1)  
Code 5311T (Mr. Hamilton) (1)  
Code 714 (Mr. Pederson) (1)  
Code 7143 (Mr. Colborn) (1)

Chief of Naval Research  
800 North Quincy Street  
Arlington, VA 22217  
Attn: Code 102B (1)  
Code 230 (Mr. Miller) (1)  
Code 480 (1)

Commander  
Naval Electronics System Command  
Washington, DC 20360  
Attn: PME 124-30 (1)  
PME 124-60 (1)

Commanding Officer  
Naval Research Laboratory  
Washington, DC 20375  
Attn: Code 8100 (1)  
Code 8160 (1)  
Code 2627 (1)

Commander  
Naval Oceanographic Office  
NSTL Station, MS 39529  
Attn: Code 3000 (1)  
Code 3100 (1)  
Code 3130 (1)  
Code 3132 (Mr. Kerling) (1)  
Code 3400 (1)  
Code 3440 (1)  
Code 3700 (1)  
Code 9100 (1)  
Code 9100 (Mr. Blumenthal) (1)  
Code 9100 (Mr. Doblar) (1)  
Library (1)

Defense Documentation Center  
Cameron Station  
Alexandria, VA 22314 (12)

Oceanographic Development Squadron 8  
Naval Air Station  
Patuxent River, MD 20670 (1)

Commanding Officer  
Naval Ocean Research & Development Activity  
NSTL Station, MS 39529  
Attn: Code 105 (1)  
Code 110 (1)  
Code 115 (1)  
Code 115 (Dr. Durham) (1)  
Code 125 (1)  
Code 300 (1)  
Code 320 (1)  
Code 340 (1)

Code 500 (1)  
Code 520 (1)  
Code 530 (1)  
Classified Library (3)

Scripps Institution of Oceanography  
Marine Physical Laboratory  
San Diego, CA 92152  
Attn: Dr. V. C. Anderson (1)

University of Texas  
Applied Research Laboratories  
P. O. Box 8029  
Austin, TX 78712  
Attn: G. E. Ellis (1)  
Dr. L. D. Hampton (1)

Woods Hole Oceanographic Institution  
Woods Hole, MA 02543  
Attn: Library (1)

University of Washington  
Department of Oceanography  
Seattle, WA 98195  
Attn: Library (1)

Director  
Naval Science Assistance Program  
Naval Surface Weapons Center  
White Oak Laboratory  
Silver Spring, MD 20910  
Attn: Code D23 (Mr. Pifer) (1)

SACLANT ASW Research Center  
Le Spezia, Italy  
Attn: Library (1)

## Unclassified

SECURITY CLASSIFICATION OF THIS PAGE (When Data Entered)

REPORT DOCUMENTATION PAGE		READ INSTRUCTIONS BEFORE COMPLETING FORM
1. REPORT NUMBER NORDA Technical Note 52	2. GOVT ACCESSION NO.	3. RECIPIENT'S CATALOG NUMBER
4. TITLE (and Subtitle) Sound Speed and Oceanic Frontal Variability in the Western Alboran Sea (January-March 1979)		5. TYPE OF REPORT & PERIOD COVERED Final
7. AUTHOR(s) Don F. Fenner		6. PERFORMING ORG. REPORT NUMBER
9. PERFORMING ORGANIZATION NAME AND ADDRESS Naval Ocean Research and Development Activity NSTL Station, Mississippi 39529		10. PROGRAM ELEMENT PROJECT TASK AREA & WORK UNIT NUMBERS 120023
11. CONTROLLING OFFICE NAME AND ADDRESS Naval Ocean Research and Development Activity Code 340 NSTL Station, Mississippi 39529		12. REPORT DATE September 1979
14. MONITORING AGENCY NAME & ADDRESS (if different from Controlling Office)		13. NUMBER OF PAGES 39
16. DISTRIBUTION STATEMENT (of this Report) Distribution Unlimited		15. SECURITY CLASS. (of this report) Unclassified
17. DISTRIBUTION STATEMENT (of the abstract entered in Block 20, if different from Report)		
18. SUPPLEMENTARY NOTES		
19. KEY WORDS (Continue on reverse side if necessary and identify by block number) Sound speed, Temperature, Salinity, Alboran Front, Anti-cyclonic Gyre, Atmospheric Pressure, Sonic Layer Depth, Deep Sound Channel, Acoustic Propagation		
20. ABSTRACT (Continue on reverse side if necessary and identify by block number) Between 26 January and 19 March 1979, nearly 250 oceanographic observations (mostly airborne expendable bathythermographs) were collected throughout the western Alboran Sea as part of a Fleet exercise. All observations were converted to sound speed using the equation of Mackenzie (1976, 1977) and a salinity field derived from historical data. A warm, anticyclonic gyre of Atlantic Water (bounded on the north and east by the Alboran Front) was encountered west of about 4°W between 26 January and 2-3 March, but was absent west of about 4°30'W on 10-11 and 19 March. Frontal zone		

Unclassified

SECURITY CLASSIFICATION OF THIS PAGE (When Data Entered)

10-11 and 19 March. Frontal zone widths varied between 3 nm (6 km) and about 20 nm (37 km). Sonic layer depth was typically 120-180 m within the anticyclonic gyre and decreased across the frontal zone to 20-60 m (maximum gradient of 16.7 m/nm or 9.0 m/km). The depth of the deep sound channel axis was typically 100-150 m within the gyre and decreased across the frontal zone to 100-150 m (maximum gradient of 15.0 m/nm or 8.3 m/km). Depth excess throughout the western Alboran Sea was more than adequate for convergence zone propagation from either a near-surface or 100 m source. Maximum temporal sound speed variability at 36°N, 4°30'W over the course of the exercise was similar in magnitude (about 125 m) to maximum spatial variability along 4°30'W (meridional section). Atmospheric forcing was observed to influence both the size and location of the anticyclonic gyre.

Unclassified

SECURITY CLASSIFICATION OF THIS PAGE (When Data Entered)